

SU(5) unification of two triplet seesaw and leptogenesis with dark matter and vacuum stability

Mina Ketan Parida^{a,*}, Riyanka Samantaray^a

^aCentre of Excellence in Theoretical and Mathematical Sciences, Siksha 'O' Anusandhan, Deemed to be University, Khandagiri Square, Bhubaneswar 751030, India

Abstract

We investigate unification prospects of two heavy scalar triplet extension of the standard model where, in the absence of any right-handed neutrino (RHN), type-II seesaw accounts for current oscillation data with hierarchical neutrino masses consistent with cosmological bounds and the lighter triplet decay explains baryon asymmetry of the Universe via leptogenesis. We note that the absence of RHNs in the fundamental fermion representations of SU(5) delineates its outstanding position compared to SO(10) (or E_6). In addition, SU(5) needs smaller scalar representations $15_{H1} \oplus 15_{H2}$ compared to much larger representations $126_{H1} \oplus 126_{H2} \subset SO(10)$ (or $351'_{H1} \oplus 351'_{H2} \subset E_6$). We show how precision gauge coupling unification is achieved through SU(5) with the predictions of different sets of two heavy triplet masses which, besides being compatible with type-II seesaw, are also consistent with unflavoured or τ -flavoured leptogenesis predictions for baryon asymmetry of the Universe. In addition to an intermediate mass colour octet fermion, completion of precision gauge coupling unification is found to require essentially the presence of the well known weak triplet fermion $\Sigma(3, 0, 1)$ in its mass range $M_\Sigma \simeq \mathcal{O}(500 - 3000)$ GeV out of which the dominant dark matter (DM) resonance mass $M_\Sigma \geq 2.4$ TeV is known to account for the observed cosmological relic density. The deficiency in relic density for the other class of lighter M_Σ solutions allowed under indirect search constraints is circumvented by the introduction of a scalar singlet DM which could be as light as 62 GeV. A GUT ansatz is noted to ensure vacuum stability of the SM scalar potential for all types of unification solutions realised in this work. We discuss proton lifetime estimations for $p \rightarrow e^+\pi^0$ compatible with the present Hyper-Kamiokande bound as a function of an unknown mixing parameter in the model.

1. Introduction

Neutrino oscillation [1–3], baryon asymmetry of the universe [4, 5], and dark matter [5–13] are the three prominent physics issues beyond the purview of the standard model (SM). Further, the origin of different strengths of strong, weak, and electromagnetic interactions in $SU(2)_L \times U(1)_Y \times SU(3)_C (\equiv G_{213})$ can not be explained by SM itself [14–19]. However, the underlying origin of neutrino masses is widely recognised to be seesaw mechanisms [20–23] some of which also explain baryon asymmetry of the Universe (BAU) via leptogenesis caused by the decay of mediating heavy scalars or fermions, and by sphaleron interactions [24]. Large number of leptogenesis models using right-handed neutrino (RHN) mediated type-I [20, 21, 25] and other seesaw mechanisms have been proposed for successful baryon asymmetry generation; a partial list of such extensive investigations has been given in [26–29] and references therein. In a novel interesting proposal [30] as an alternative mechanism without RHNs, realization of neutrino masses and baryon asymmetry of the Universe (BAU) has been shown to be possible [31–34] through the SM extension by two heavy scalar triplets, $\Delta_1(3, -1, 1)$ and $\Delta_2(3, -1, 1)$ of identical G_{213} charges, each of which also generates neutrino mass by type-II seesaw [22]. The tree level dilepton decay of any one of these triplets combined with loop contribution generated by their collaboration predicts the desired CP-asymmetry formula for leptogenesis

*Corresponding author

Email addresses: minaparida@soa.ac.in (Mina Ketan Parida), riyankasamantaray59@gmail.com (Riyanka Samantaray)

leading to observed baryon asymmetry of the Universe.

Very recently, as a departure from the proposed applicability to quasi-degenerate neutrinos [30], we have shown [34] the success of the two triplet model (TTM) in following respects: The model explains current neutrino data [1–3] comprising of atmospheric neutrino mixing in the second octant, large Dirac CP phases, and hierarchical neutrino masses of both normal and inverted orderings. The model has been also found to be consistent with the cosmological bound $\Sigma_{(2015)}$ on the sum of three neutrino masses derived using the Planck satellite data [5] as well as the improved bound $\Sigma_{(2018)}$ [35–37]

$$\Sigma_{(2015)} = \sum_{i=1}^3 \hat{m}_i \leq 0.23 \text{ eV}; \quad \Sigma_{(2018)} = \sum_{i=1}^3 \hat{m}_i \leq 0.12 \text{ eV}. \quad (1)$$

Additional sources of CP-asymmetry of TTM have been exploited to further predict the BAU in the cases of unflavoured and partially flavoured ($\equiv \tau$ -flavoured) leptogenesis covering lighter triplet mass $M_{\Delta_2} \simeq \mathcal{O}(10^{10} - 10^{14})$ GeV and the corresponding values of heavier triplet masses $M_{\Delta_1} \geq 10M_{\Delta_2}$ [34]. Moreover, the two triplet model (TTM) has been shown to possess an inbuilt fine tuning mechanism to keep the standard Higgs mass safe against radiative instability [34]. With additional Z_2 stabilising discrete symmetry, the model has also successfully addressed issues on dark matter (DM) and vacuum stability with the prediction of a scalar DM mass ~ 1.3 TeV which also ensures radiative stability of the standard Higgs scalar mass [34].

In this work, for the first time, we implement unification of three gauge couplings of the two triplet model (TTM) which has been left unanswered so far. New origins of CP-asymmetry in hybrid seesaw [27] and in type-II seesaw dominated single-triplet leptogenesis model empowered by RHN loop mediation have been successfully addressed in SO(10) [19, 28]. Triplet seesaw dominance has been shown to predict $\nu_\mu - \nu_\tau$ mixing in SUSY GUTs [38, 39] as well as three neutrino mixings [40] and fermion masses in SO(10) [41, 42]. Also there are interesting investigations in left-right symmetric models or in SM extensions with or without dark matter [43–51].

As SO(10) [16] and E_6 [17, 52] fundamental fermion representations intrinsically contain RHNs, in this work we search for an alternative GUT since the TTM is based upon the unconventional novel hypothesis that the origin of neutrino masses as well as BAU generation do not need RHNs. However, the SU(5) theory [15, 53–55] does not have RHNs in its fundamental fermion representations: $10_F \oplus \bar{5}_F$ which exactly complete the SM fermions. We would like to emphasize that, unlike the SU(5) models occurring as intermediate symmetry in SO(10)(or E_6) \rightarrow SU(5) \rightarrow SM [28, 56, 57], here we utilise the independent class of SU(5) models [15, 53–55]. Hybrid seesaw near TeV scale mediated by triplet and singlet fermions has been implemented proposing interesting experimental signature at LHC [58]. Noting further that a scalar triplet $\Delta(3, -1, 1)$ is contained in the representation 15_H of SU(5), or in 126_H of SO(10) (or in $351'_H$ of E_6), the embedding of the two scalar triplets requires much smaller SU(5) scalar representations $15_{H1} \oplus 15_{H2}$ compared to far more larger representations $126_{H1} \oplus 126_{H2} \subset SO(10)$ and $351'_{H1} \oplus 351'_{H2} \subset E_6$. We show how such a SU(5) GUT framework [15] predicts all the ingredients of the TTM [34] with gauge unification of strong, weak, and electromagnetic interactions. Interestingly, the completion of coupling unification is found to predict the well known non-standard fermion triplet $\Sigma(3, 0, 1)$ as an important component of WIMP dark matter [59–65] where vacuum stability of the SM Higgs scalar potential is ensured by an intermediate mass scalar singlet threshold effect [66]. Proton lifetime formula in this class of SU(5) contains an unknown mixing parameter [54, 55] whose allowed range in the present TTM unification realization is only partially accessed by the current Super-Kamiokande [67] or Hyper-Kamiokande search limits [68]. Highlights of the present work are

- The absence of RHN in the fundamental fermion representation of SU(5) compared to SO(10) and E_6 is noted to identify the minimal rank-4 GUT as a natural candidate to unify the two-triplet model (TTM). In addition, this SU(5) embedding of TTM requires smaller scalar representations $15_{H1} \oplus 15_{H2}$ compared to much larger representations $126_{H1} \oplus 126_{H2}$ of SO(10), or $351'_{H1} \oplus 351'_{H2}$ of E_6 .
- Renormalisation group (RG) predicted successful embedding of the two triplet model in SU(5) grand unified theory with precision gauge coupling unification at $M_U \simeq \mathcal{O}(10^{15})$ GeV.
- Unification prediction of all the sets of two heavy scalar triplet masses [34] in the range $\mathcal{O}(10^{10})$ GeV $< M_{\Delta_2} < M_{\Delta_1} \leq M_U$ ensuring type-II seesaw ansatz for neutrino oscillation data fitting and baryon asymmetry prediction

through unflavoured or τ -flavoured leptogenesis [34].

- In addition to an intermediate mass colour octet fermion, the unification completion is found to predict essentially a fermionic triplet dark matter $\Sigma(3, 0, 1)$ [59, 61, 64, 65] in its mass range $M_\Sigma \simeq \mathcal{O}(500 - 3000)$ GeV out of which dominant minimal thermal DM with resonance mass $M_\Sigma = 2.4$ TeV, or heavier, accounts for the entire observed value of cosmological relic density.
- In the other class of lighter fermionic triplet sub-dominant DM mass solutions, $M_\Sigma \simeq \mathcal{O}(500 - 2000)$ GeV, permitted by indirect search constraints, the model is shown to account for the observed DM relic density through the introduction of a scalar singlet DM ξ whose mass could be as light as $m_\xi \simeq 62$ GeV.
- An intermediate mass Higgs scalar singlet threshold effect originating from SU(5) breaking is noted to ensure vacuum stability of the SM scalar potential for all classes of allowed solutions emerging from this GUT realization.
- In view of an unknown mixing parameter that occurs in the proton decay formula for $p \rightarrow e^+\pi^0$ in this class of SU(5) models [54, 55], the present Hyper-Kamiokande limit [68] is capable of constraining only a limited region of this parameter space.

This paper is organised in the following manner. In Sec.2 we briefly summarise the recent work on two triplet model without grand unification [34]. Sec. 3 elucidates our new implementation and unification results in SU(5) GUT framework including Δ_1, Δ_2 mass predictions required for neutrino mass fits and unflavoured or τ -flavoured leptogenesis. In Sec.4.2, we discuss proton lifetime estimations in this SU(5) model. Sec.5 deals with $SU(5) \times Z_2$ ansatz for fermionic triplet dark matter (DM) and its prospects and limitations. Vacuum stability of the SM scalar potential is discussed in Sec.5.0.4. The model capability to accommodate fermionic triplet plus scalar singlet DM is discussed in Sec.6. Grand unification advantage over ununified TTM in predicting fermionic triplet or scalar singlet DM and vacuum stability are briefly discussed in Sec. 7. We summarize and conclude in Sec.8. In Sec.10.1 of Appendix a brief discussion is made on non-standard fermion masses.

2. The two triplet model for neutrino mass and leptogenesis

In this section we briefly summarise the outcome of the two-triplet model [34] relevant for the present embedding in SU(5) grand unification.

2.1. Neutrino masses and mixings through type-II seesaw

The SM is extended by the addition of two heavy scalar triplets $\Delta_1(3, -1, 1)$ and $\Delta_2(3, -1, 1)$ with masses M_{Δ_1} and M_{Δ_2} , respectively. Here respective charges have been indicated under the SM gauge group $SU(2)_L \times U(1)_Y \times SU(3)_C$. The extended part of the Lagrangian that contributes to type-II seesaw generation of neutrino masses and leptogenesis is

$$\begin{aligned}
-\mathcal{L}_{ext} = & \sum_{\alpha=1}^2 \left((D_\mu \vec{\Delta}_\alpha)^\dagger \cdot (D^\mu \vec{\Delta}_\alpha) - M_{\Delta_\alpha}^2 \text{Tr}(\Delta_\alpha^\dagger \Delta_\alpha) \right) \\
& + \sum_{\alpha=1}^2 \left(\left[\frac{1}{2} \sum_{ij} f_{ij}^{(\alpha)} L_i^T C i \tau_2 \Delta_\alpha L_j - \mu_{\Delta_\alpha} \phi^T i \tau_2 \Delta_\alpha \phi + h.c. \right] \right). \quad (2)
\end{aligned}$$

Here the three lepton doublets are $L_i (i = 1, 2, 3)$, $\alpha = 1, 2$ denote the two scalar triplets, M_{Δ_α} = mass of the triplet Δ_α , $f_{ij}^{(\alpha)}$ = Majorana coupling of Δ_α with L_i and L_j , and μ_{Δ_α} = lepton-number violating (LNV) trilinear coupling of Δ_α with standard Higgs doublet ϕ . The induced VEVs, $V_{\Delta_\alpha} (\alpha = 1, 2)$, parameterizing neutrino mass matrix m_ν , are

$$V_{\Delta_\alpha} = \frac{\mu_{\Delta_\alpha} v^2}{2M_{\Delta_\alpha}^2}, (\alpha = 1, 2), \quad (3)$$

$$\begin{aligned}
m_\nu &= 2f^{(1)}V_{\Delta_1} + 2f^{(2)}V_{\Delta_2}, \\
&= f^{(1)}\frac{\mu_{\Delta_1}v^2}{M_{\Delta_1}^2} + f^{(2)}\frac{\mu_{\Delta_2}v^2}{M_{\Delta_2}^2} \\
&\equiv m_\nu^{(1)} + m_\nu^{(2)}.
\end{aligned} \tag{4}$$

Here $v = 246$ GeV = the standard Higgs vacuum expectation value (VEV). The neutrino data are fitted using the PDG convention [69] on the PMNS mixing matrix

$$U_{\text{PMNS}} = \begin{pmatrix} c_{12}c_{13} & s_{12}c_{13} & s_{13}e^{-i\delta} \\ -s_{12}c_{23} - c_{12}s_{23}s_{13}e^{i\delta} & c_{12}c_{23} - s_{12}s_{23}s_{13}e^{i\delta} & s_{23}c_{13} \\ s_{12}s_{23} - c_{12}c_{23}s_{13}e^{i\delta} & -c_{12}s_{23} - s_{12}c_{23}s_{13}e^{i\delta} & c_{23}c_{13} \end{pmatrix} \text{diag}(e^{i\frac{\alpha_M}{2}}, e^{i\frac{\beta_M}{2}}, 1), \tag{5}$$

where $s_{ij} = \sin \theta_{ij}$, $c_{ij} = \cos \theta_{ij}$ with $(i, j = 1, 2, 3)$, δ is the Dirac CP phase and (α_M, β_M) are Majorana phases. The best fit values of the oscillation data [2, 3] summarised below in Table 1 have been used in [34].

Table 1: Input data from neutrino oscillation experiments [2, 3]

Quantity	best fit values	3σ ranges
Δm_{21}^2 [$10^{-5}eV^2$]	7.39	6.79 – 8.01
$ \Delta m_{31}^2 $ [$10^{-3}eV^2$](NO)	2.52	2.427 – 2.625
$ \Delta m_{32}^2 $ [$10^{-3}eV^2$](IO)	2.51	2.412 – 2.611
$\theta_{12}/^\circ$	33.82	31.61 – 36.27
$\theta_{23}/^\circ$ (NO)	49.6	40.3 – 52.4
$\theta_{23}/^\circ$ (IO)	49.8	40.6 – 52.5
$\theta_{13}/^\circ$ (NO)	8.61	8.22 – 8.99
$\theta_{13}/^\circ$ (IO)	8.65	8.27 – 9.03
$\delta/^\circ$ (NO)	215	125 – 392
$\delta/^\circ$ (IO)	284	196 – 360

Important features of the data are: (i) atmospheric mixing angle θ_{23} in the second octant, (ii) large values of Dirac CP phases exceeding $\delta = 200^\circ$, (iii) includes the reactor neutrino mixing $\theta_{13} = 8.6^\circ$ determined earlier. Denoting the mass eigen values as $\hat{m}_i (i = 1, 2, 3)$ and the relation

$$m_\nu = U_{\text{PMNS}} \text{diag}(\hat{m}_1, \hat{m}_2, \hat{m}_3)U_{\text{PMNS}}^T, \tag{6}$$

all the nine elements of the symmetric matrix m_ν for NO and IO type hierarchies including mass eigen values are given in Table 2.

The best fits in both the NO and IO cases satisfy the current cosmological bounds of eq.(1) on the sum of three neutrino masses which have been derived using the Planck satellite data and the Λ CDM [5, 35] big-bang cosmology.

2.2. CP-asymmetry

In the interaction Lagrangian in eq.(2), lepton number violation (LNV) occurs due to the coexistence of the Higgs triplet-bilepton Yukawa matrix f along with the trilinear couplings μ_{Δ_α} ($\alpha = 1, 2$). In the absence of heavy RHNs, the entire CP asymmetry is due to the decay of the two heavy scalar triplets. At tree level the scalar triplets can decay to bileptons or to SM Higgs with the corresponding branching ratios

$$B_l^\alpha = \sum_{i=e,\mu,\tau} B_{l_i}^\alpha = \sum_{i,j=e,\mu,\tau} B_{l_{ij}}^\alpha = \sum_{i,j=e,\mu,\tau} \frac{M_{\Delta_\alpha}}{8\pi\Gamma_{\Delta_\alpha}^{\text{tot}}} |f_{ij}^{(\alpha)}|^2 \text{ and} \tag{7}$$

$$B_\phi^\alpha = \frac{|\mu_{\Delta_\alpha}|^2}{8\pi M_{\Delta_1} \Gamma_{\Delta_\alpha}^{\text{tot}}}, \tag{8}$$

Table 2: Neutrino mass matrices and eigen values in NO and IO hierarchies from oscillation data .

Quantity	Best fit values
$(m_\nu)_{ij}(\text{eV})(\text{NO})$	$\begin{pmatrix} 0.00367 - 0.00105i & -0.00205 + 0.00346i & -0.00634 + 0.00294i \\ -0.00205 + 0.00346i & 0.03154 + 0.00034i & 0.02106 - 0.0001i \\ -0.00634 + 0.00294i & 0.02106 - 0.0001i & 0.02383 - 0.00027i \end{pmatrix}$
$(m_\nu)_{ij}(\text{eV})(\text{IO})$	$\begin{pmatrix} 0.0484 - 0.00001i & -0.001122 + 0.0055i & -0.00137 + 0.00471i \\ -0.001122 + 0.0055i & 0.02075 - 0.00025i & -0.02459 - 0.00026i \\ -0.00137 + 0.00471i & -0.02459 - 0.00026i & 0.02910 - 0.00026i \end{pmatrix}$
$\hat{m}_i(\text{eV})(\text{NO})$	diag(0.001, 0.0086, 0.0502)
$\hat{m}_i(\text{eV})(\text{IO})$	diag(0.0493, 0.0501, 0.0010)
$\sum_{(i=1)}^3 \hat{m}_i(\text{eV})(\text{NO})$	0.0598
$\sum_{(i=1)}^3 \hat{m}_i(\text{eV})(\text{IO})$	0.1000

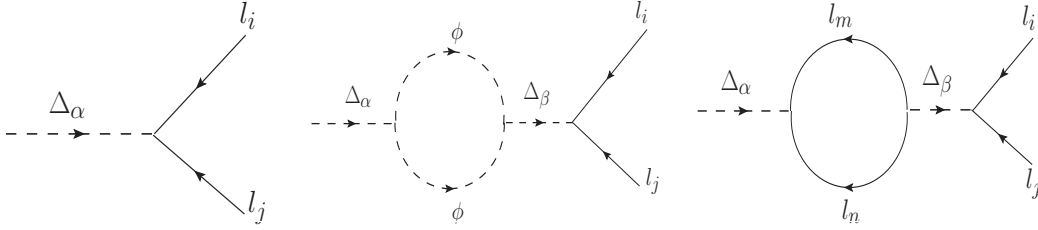


Figure 1: Tree level and one loop Feynman diagrams for a triplet decaying to bi-leptons in case of flavoured leptogenesis.

which satisfy $B_l^\alpha + B_\phi^\alpha = 1$. Here $\Gamma_{\Delta_\alpha}^{tot}$ is the total decay width of Δ_α

$$\Gamma_{\Delta_\alpha}^{tot} = \frac{M_{\Delta_\alpha}}{8\pi} \left(\sum_{i,j} |f_{ij}^{(\alpha)}|^2 + \frac{|\mu_{\Delta_\alpha}|^2}{M_{\Delta_\alpha}^2} \right). \quad (9)$$

The decay to bi-leptons also occurs due to loop mediation caused by either the SM Higgs or the leptons as shown in Fig.1. The CP-asymmetry which arises due to the interference of the tree level and one-loop contributions consists of two pieces: (i) the scalar loop generated asymmetry denoted by \mathcal{L}, \mathcal{F} which violates both lepton number and flavour, (ii) the lepton loop generated flavour only violating asymmetry denoted by \mathcal{F} [32, 34]

$$\epsilon_{\Delta_\alpha}^{l_i} = \epsilon_{\Delta_\alpha}^{l_i(\mathcal{L}, \mathcal{F})} + \epsilon_{\Delta_\alpha}^{l_i(\mathcal{F})}. \quad (10)$$

The indices n, i in the above expressions of CP asymmetries stand for the lepton flavour indices (e, μ, τ). It is thus realised that when summed over flavour indices, the second piece of the CP asymmetry arising solely out of flavour violation vanishes identically, i.e

$$\sum_{i=e,\mu,\tau} \epsilon_{\Delta}^{l_i(\mathcal{F})} = 0. \quad (11)$$

This CP asymmetry parameter survives only in the case of flavoured leptogenesis. Since this asymmetry does not involve any lepton number violation, it is also called purely flavoured asymmetry and the corresponding leptogenesis scenario which is dominated by the flavour violating CP asymmetry ($\epsilon_{\Delta}^{l_i(\mathcal{F})} \gg \epsilon_{\Delta}^{l_i(\mathcal{L}, \mathcal{F})}$) is referred to as purely flavoured (PFL) leptogenesis. The condition for PFL leptogenesis is [32]

$$\mu_{\Delta_2}^* \mu_{\Delta_1} \ll M_{\Delta_2}^2 \text{Tr}(f^{(2)} f^{(1)\dagger}). \quad (12)$$

Consistent with dominance of $m_\nu^{(2)}$ over $m_\nu^{(1)}$ and the condition that $M_{\Delta_2} < M_{\Delta_1} \simeq \mu_{\Delta_1}$, PFL condition has not been guaranteed in our flavoured leptogenesis regime [34].

Leptogenesis guided Δ_2 -seesaw dominance:

Utilisation is made of the cosmological principle that the decay of the lower mass triplet Δ_2 with $M_{\Delta_2} \ll M_{\Delta_1}$ generates the dominant asymmetry surviving the Hubble expansion rate of the universe as it erases out the asymmetry caused by the decay of the heavier triplet Δ_1 . This leads to the CP-asymmetry dominance by the decay of Δ_2 . More profoundly, the inequality $M_{\Delta_2} \ll M_{\Delta_1}$ also predicts type-II seesaw dominance of neutrino mass matrix by $m_\nu^{(2)}$ mediated by Δ_2 . From the behaviour of two respective neutrino mass matrices and induced VEVs, $m_\nu^{(1)} \propto V_{\Delta_1}$, $m_\nu^{(2)} \propto V_{\Delta_2}$, $V_{\Delta_1} \propto \frac{1}{M_{\Delta_1}^2}$, $V_{\Delta_2} \propto \frac{1}{M_{\Delta_2}^2}$, the leptogenesis guided principle requiring $M_{\Delta_2} \ll M_{\Delta_1}$ predicts

$$\begin{aligned} m_\nu^{(1)} &\ll m_\nu^{(2)}, \\ m_\nu &= m_\nu^{(1)} + m_\nu^{(2)} \simeq m_\nu^{(2)} = m_\nu^{\text{DATA}}. \end{aligned} \quad (13)$$

This determines all the elements of the mass matrix $m_\nu^{(2)}$ from best fits to neutrino data given in Table 2.

For the sake of simplicity ignoring the scalar triplet index and denoting $\Delta_2 \equiv \Delta$ result in $\epsilon_\Delta \equiv \epsilon_{\Delta_2}$, $B_l \equiv B_l^2$, $B_\phi \equiv B_\phi^2$. Then the two pieces of CP asymmetry in eq.(10) arising due to Δ_2 decay are

$$\epsilon_\Delta^{l_i(\mathcal{L}, \mathcal{F})} = \frac{1}{2\pi} \frac{\text{Im} \left\{ \sum_n (f^{(2)})_{ni}^* (f^{(1)})_{ni} \mu_{\Delta_2}^* \mu_{\Delta_1} \right\}}{M_{\Delta_2}^2 \text{Tr}(f^{(2)} f^{(2)\dagger}) + |\mu_{\Delta_2}|^2} g(x_{12}), \quad (14)$$

$$\epsilon_\Delta^{l_i(\mathcal{F})} = \frac{1}{2\pi} \frac{\text{Im} \left\{ (f^{(2)\dagger} f^{(1)})_{ii} \text{Tr}(f^{(2)} f^{(1)\dagger}) \right\}}{M_{\Delta_2}^2 \text{Tr}(f^{(2)} f^{(2)\dagger}) + |\mu_{\Delta_2}|^2} g(x_{12}), \quad (15)$$

where

$$\begin{aligned} g(x_{\alpha\beta}) &= \frac{x_{\alpha\beta}(1 - x_{\alpha\beta})}{(1 - x_{\alpha\beta})^2 + x_{\alpha\beta}y}, \\ x_{\alpha\beta} &= \frac{M_{\Delta_\alpha}^2}{M_{\Delta_\beta}^2}, \\ y &= \left(\frac{\Gamma_{\Delta_\beta}^{\text{tot}}}{M_{\Delta_\beta}} \right)^2. \end{aligned} \quad (16)$$

The indices n, i in the above expressions of CP asymmetries stand for the lepton flavour indices (e, μ, τ). It has been shown that purely flavoured leptogenesis [32] is not possible in the two-triplet seesaw model [34]. The recent neutrino oscillation data are fitted using the leptogenesis guided Δ_2 -seesaw dominance with $M_{\Delta_2} \ll M_{\Delta_1}$

$$m_\nu \simeq m_\nu^{(2)} = m_\nu^{\text{DATA}}. \quad (17)$$

Noting that the mass matrices $m_\nu^{(1)}$ and $m_\nu^{(2)}$ can always be represented as

$$\begin{aligned} (m_\nu^{(1)})_{ij} &= |m_\nu^{(1)}{}_{ij}| e^{i\psi_{ij}^{(1)}}, \\ (m_\nu^{(2)})_{ij} &= |m_\nu^{(2)}{}_{ij}| e^{i\psi_{ij}^{(2)}}, \end{aligned} \quad (18)$$

gives

$$\begin{aligned} \frac{(m_\nu^{(1)})_{ij}}{(m_\nu^{(2)})_{ij}} &= \frac{|m_\nu^{(1)}{}_{ij}|}{|m_\nu^{(2)}{}_{ij}|} e^{i\phi_{ij}}, \\ &= G_{ij} e^{i\phi_{ij}}. \end{aligned} \quad (19)$$

where

$$\begin{aligned}\phi_{ij} &= \psi_{ij}^{(1)} - \psi_{ij}^{(2)}, \\ G_{ij} &= \frac{|(m_\nu^{(1)})_{ij}|}{|(m_\nu^{(2)})_{ij}|}.\end{aligned}\quad (20)$$

Then each element of $m_\nu^{(1)}$ is connected to the corresponding element of $m_\nu^{(2)}$ through a multiplicative factor which is a complex number

$$(m_\nu^{(1)})_{ij} = G_{ij} e^{i\phi_{ij}} (m_\nu^{(2)})_{ij} \quad (21)$$

In the unflavoured regime the lighter triplet mass has the lowest limit $M_{\Delta_2} \gtrsim 4 \times 10^{11}$ GeV [34]. Partially flavoured- or τ - flavoured leptogenesis (equivalent to $e + \mu$ flavoured-leptogenesis) has been found to be successful for $M_{\Delta_2} \simeq (10^{10} - 10^{11})$ GeV [34]. In the unflavoured regime, the purely flavoured CP asymmetry part vanishes leading to non-vanishing lepton number plus flavour violating parts which have been represented in terms of the experimental value of $m_\nu (= m_\nu^{\text{DATA}})$,

$$\begin{aligned}\epsilon_\Delta^l &= \sum_i \epsilon_\Delta^{l(L,F)} \\ &= \frac{M_{\Delta_1}^2 M_{\Delta_2}^2}{2\pi v^4} \frac{\sum_{ij} G_{ij} |(m_\nu)_{ij}|^2 \sin(\psi_{ij}^{(1)} - \psi_{ij}^{(2)})}{M_{\Delta_2}^2 \text{Tr}(f^{(2)} f^{(2)\dagger)} + |\mu_{\Delta_2}|^2} g(x_{12})\end{aligned}\quad (22)$$

$$\simeq \frac{M_{\Delta_1}^2 M_{\Delta_2}^2}{16\pi^2 v^4} \frac{\sum_{ij} G_{ij} |(m_\nu)_{ij}|^2 \sin(\psi_{ij}^{(1)} - \psi_{ij}^{(2)})}{(M_{\Delta_1}^2 - M_{\Delta_2}^2)} \left(\frac{M_{\Delta_2}}{\Gamma_{\Delta_2}^{\text{tot}}} \right).\quad (23)$$

Then for $M_{\Delta_1} \gg M_{\Delta_2}$, the CP-asymmetry is

$$\begin{aligned}\epsilon_\Delta^l &= \frac{M_{\Delta_2}^2}{16\pi^2 v^4} \sum_{ij} G_{ij} |(m_\nu)_{ij}|^2 \sin(\psi_{ij}^{(1)} - \psi_{ij}^{(2)}) \left(\frac{M_{\Delta_2}}{\Gamma_{\Delta_2}^{\text{tot}}} \right) \\ &\equiv \frac{M_{\Delta_2}^2}{16\pi^2 v^4} \sum_{ij} G_{ij} |(m_\nu)_{ij}|^2 \sin(\phi_{ij}) \left(\frac{M_{\Delta_2}}{\Gamma_{\Delta_2}^{\text{tot}}} \right).\end{aligned}\quad (24)$$

Out of 9 elements of the ratio G_{ij} , or the phase differences ϕ_{ij} , only 6 are independent which have been used as input to CP-asymmetry through the functions

$$\begin{aligned}F &= (G_{11}, G_{22}, G_{33}, G_{12}, G_{13}, G_{23}), \\ \Phi &= (\phi_{11}, \phi_{22}, \phi_{33}, \phi_{12}, \phi_{13}, \phi_{23}).\end{aligned}\quad (25)$$

For the sake of simplicity, a common magnitude ratio has been fixed for different varieties of leptogenesis solutions[34]

$$F = (0.1, 0.1, 0.1, 0.1, 0.1, 0.1), \quad (26)$$

which ensures Δ_2 seesaw dominance.

For phase differences between the corresponding elements of $m_\nu^{(1)}$ and $m_\nu^{(2)}$ we have used two different possibilities for every numerical computation:

(i) Fixed phase difference:

$$\Phi = (-\pi/2, -\pi/2, -\pi/2, -\pi/2, -\pi/2, -\pi/2), \quad (27)$$

(ii) Randomised phase difference:

$$\frac{\Phi}{\pi} = (-0.3418, -0.0807, 0.7850, 0.9961, -0.4427, 0.7244) \quad (28)$$

where the assumption in eq.(27) has been made to yield maximal CP-asymmetry as input to flavoured Boltzmann equations, but the more generalised phase differences of eq.(28) has been suggested through random number generation [34]. Using the CP-asymmetry thus predicted by two-triplet seesaw model from neutrino data as input, the respective sets of coupled Boltzmann equations have been solved in different cases to predict the desired baryon asymmetry of the Universe [34] defined through Y_B or η_B given below.

$$Y_B = \frac{n_B - n_{\bar{B}}}{s}. \quad (29)$$

Here $n_B, n_{\bar{B}}$ are number densities of baryons and anti-baryons, respectively, and s is the entropy density.

$$\eta_B = \frac{n_B - n_{\bar{B}}}{n_\gamma}, \quad (30)$$

were $n_\gamma =$ photon density. Planck satellite experimental values are[5]

$$Y_B = 8.66 \pm 0.11 \times 10^{-11}, \quad (31)$$

$$\eta_B = 6.10 \pm 0.08 \times 10^{-10}. \quad (32)$$

Our estimations of BAU [34] have been found to match with the Planck satellite experimental values given in eq.(31) and eq.(32). The masses of triplets, trilinear couplings, types of neutrino mass hierarchy and phase difference Φ/π which have yielded successful predictions of BAU used and the corresponding leptogenesis type in each case have been summarised in Table 3.

Table 3: Scalar triplet masses and lepton number violating couplings of the two-triplet model leading to baryon asymmetry prediction through leptogenesis in concordance with current neutrino data and cosmological bounds for NO and IO type mass hierarchies [34].

M_{Δ_1} (GeV)	μ_{Δ_1} (GeV)	M_{Δ_2} (GeV)	μ_{Δ_2} (GeV)	Hierarchy type	Leptogenesis type	Phase difference
3×10^{13}	10^{13}	10^{12}	2.4×10^{10}	NO	Unflavoured	Fixed
3×10^{13}	10^{13}	10^{12}	2.0×10^{10}	IO	Unflavoured	Fixed
3×10^{13}	10^{13}	5×10^{12}	2.6×10^{11}	NO	Unflavoured	Random
3×10^{13}	10^{13}	5×10^{12}	2.1×10^{11}	IO	Unflavoured	Random
3×10^{12}	10^{12}	10^{11}	3.6×10^9	NO	τ -flavoured	Random
3×10^{12}	10^{12}	10^{11}	3.2×10^9	IO	τ -flavoured	Random

In addition to the masses of the two scalar triplets given in Table 3, we have checked that partially flavoured or two-flavoured ($\equiv \tau$ -flavoured) leptogenesis is also possible with desired BAU prediction for mass parameters $M_{\Delta_1} \simeq \mathcal{O}(10^{11})$ GeV, $M_{\Delta_2} \simeq \mathcal{O}(10^{10})$ GeV, $\mu_{\Delta_1} \simeq \mathcal{O}(10^{10})$ GeV, and $\mu_{\Delta_2} \simeq \mathcal{O}(10^9)$ GeV with NO type neutrino mass hierarchy and randomised values of the phase differences. In particular this lighter Δ_2 mass $M_{\Delta_2} \sim \mathcal{O}(10^{10})$ GeV (not shown in Table 3) is approximately estimated lowest bound on the scale for viable τ -flavoured leptogenesis.

3. Unification through SU(5)

3.1. Lighter fermions and scalars

Embedding the two-Higgs triplets in SO(10) (or E_6) GUT would result in additional contributions due to RHN mediation for both neutrino masses and BAU via leptogenesis which could destroy the special property of the TTM that both neutrino masses and leptogenesis need no RHNs [30, 34]. On the other hand all the standard fermions of one generation are contained in two fundamental SU(5) representations, $\bar{5}_F \oplus 10_F$, whose decompositions under SM gauge theory G_{213} are

$$\begin{aligned} \bar{5}_F &\supset l_L(2, -1/2, 1) + d_R(1, -1/3, 3), \\ 10_F &\supset Q_L(2, 1/6, 3) + u_R(1, 2/3, 3) + e_R(1, -1, 1). \end{aligned} \quad (33)$$

Thus like the SM, the minimal SU(5) theory does not have RHNs among its nontrivial fermion representations. This qualifies SU(5) as a suitable framework to unify the two triplet model. Another explicit advantage over GUTs of higher rank is due to much smaller size of the required SU(5) Higgs representations $15_{H1} \supset \Delta_1$ and $15_{H2} \supset \Delta_2$. Noting that the same two triplets are contained in the two scalar representations $126_{H1} \oplus 126_{H2}$ of SO(10) (or $351'_{H1} \oplus 351'_{H2} \subset E_6$), it is evident that the two scalar representations needed in SU(5) for the TTM embedding are much smaller compared to the corresponding representations of SO(10) (or E_6).

Type-II seesaw and proton decay in SU(5) using 15_H have been addressed [70] which need lepto-quark scalar masses $O(1)$ TeV. As discussed below, such scalar leptoquarks in 15_{H1} of the present TTM embedding having masses $\gg 10^{10}$ GeV, do not make any substantial contribution to proton decay [28, 71]. As SU(5) does not permit any intermediate gauge symmetry [18], gauge coupling unifications have been suggested by populating the grand desert through non-standard fermions or scalars, or both types of fields [54, 55, 57, 58, 61, 64, 65, 72–75]. The present gauge coupling unification method must be through inclusion of possible additional fields in such a way that the heavy masses of two triplets Δ_1 and Δ_2 are separated by at least one order [34]. For later use in this section we decompose the scalar (H) and fermion (F) representations of the SU(5) under G_{213} gauge group [52]

$SU(5) \supset SU(2)_L \times U(1)_Y \times SU(3)_C (\equiv G_{213})$:

$$\begin{aligned}
5_H &\supset \phi(2, 1/2, 1) + (1, -1/3, 3), \\
15_{H1} &\supset \Delta_1(3, -1, 1) + (2, 1/6, 3) + (1, 2/3, 6), \\
15_{H2} &\supset \Delta_2(3, -1, 1) + (2, 1/6, 3) + (1, 2/3, 6), \\
24_H &\supset S_{24}(1, 0, 1) + (1, 3, 0) + (1, 0, 8) + (2, -5/6, 3) + (2, 5/6, \bar{3}), \\
24_F &\supset \Sigma(3, 0, 1) + C_F(1, 0, 8)_F + S_F(1, 0, 1)_F \\
&\quad + (LQ)_F(2, -5/6, 3)_F + \overline{LQ}_F(2, 5/6, \bar{3})_F.
\end{aligned} \tag{34}$$

We have embedded the two Higgs triplets Δ_1 and Δ_2 in the SU(5) representations 15_{H1} and 15_{H2} , respectively. Here $\phi(2, 1/2, 1) \subset 5_H$ is the standard Higgs doublet. The scalar singlet $S_{24} \subset 24_H$ is usually exploited to break SU(5) \rightarrow SM. Extended survival hypothesis applies under minimal fine tuning [76, 77] to maintain gauge hierarchy resulting in only the SM Higgs doublet ϕ to be at the electroweak scale. All other scalars not needed for electroweak symmetry breaking acquire masses at the GUT scale M_U under minimal fine tuning hypothesis [76, 77]. But since two lighter scalar triplets are needed for neutrino mass and BAU ansatz [34], additional fine tuning is needed for such realizations. However, the present unification model is found to operate if all the component masses of the complete multiplet 15_{H1} can be identified with the heavier triplet mass scale $M_{15_{H1}} = M_{\Delta_1}$, an interesting criteria which has been exploited for unification in SUSY [56], split-SUSY [57] and non-SUSY [19, 28] cases. For implementation of this criteria it is necessary to realize unification of SM gauge couplings with all other necessary particle masses lighter than $M_{\Delta_1} = M_{15_{H1}}$ [56]. In a straightforward manner the mass of $\Delta_2 \subset 15_{H2}$ can be made lighter than the GUT scale by using the SU(5) invariant potential

$$\begin{aligned}
V_{15_{H2}} &= M_{15_{H2}}^2 15_{H2}^\dagger 15_{H2} + \lambda_{15_{H2}} (15_{H2}^\dagger 15_{H2})^2 + m_{(24,15_{H2})} 15_{H2}^\dagger 24_H 15_{H2} \\
&\quad + \gamma_2 Tr(24_H^2) 15_{H2}^\dagger 15_{H2} + \delta_2 15_{H2}^\dagger 24_H^2 15_{H2} + m_{(15_{H2}, 5_H)} 15_{H2} 5_H 5_H \dots
\end{aligned} \tag{35}$$

When the symmetry breaking SU(5) \rightarrow SM occurs through VEV

$$\langle S_{24H} \rangle = \frac{V_U}{\sqrt{30}} \text{diag}(2, 2, 2, -3, -3), \tag{36}$$

we get for the mass squared term for Δ_2

$$M_{\Delta_2}^2 = M_{15_{H2}}^2 - \frac{3m_{(24,15_{H2})}V_U}{\sqrt{30}} + \frac{3}{10}\lambda_{(24,15_{H2})}V_U^2 + \gamma_2 V_U^2 + \frac{3}{10}\delta_2 V_U^2, \tag{37}$$

where $M_{15_{H2}}, m_{(24,15_{H2})}$ and V_U are $\sim O(M_U)$. Then it is clear that there is ample scope to make $M_{\Delta_2}^2 \ll M_U^2$ by fine tuning of parameters in eq.(37).

In Sec. 2.1 the LNV couplings occurring in eq.(2) originate from the two trilinear SU(5) invariant couplings,

$m_{(15H_i, 5_H)} 15_{H_i} 5_H 5_H \supset \mu_{\Delta_i} \Delta_i \phi \phi (i = 1, 2)$ whose numerical values have been shown in Table 3, Table 6, and Table 7.

Besides the Higgs scalar triplets needed for neutrino mass and leptogenesis, as we show below, completion of gauge coupling unification also needs the fermion triplet $\Sigma(3, 0, 1) \subset 24_F$ and the colour octet fermion $C_F(1, 0, 8) \subset 24_F$ to be substantially lighter than the GUT scale with masses $M_\Sigma \sim \mathcal{O}(500 - 3000)$ GeV and $M_{C_F} \sim \mathcal{O}(10^8 - 10^9)$ GeV, respectively. For making non-standard fermions Σ and C_F lighter, we utilise the most convenient Yukawa Lagrangian including both normalizable as well as non-renormalizable (NR) terms [74]

$$\begin{aligned} \mathcal{L}_{NR} &= M_F \text{Tr}(24_F^2) + Y_{24} \text{Tr}(24_F^2 24_H) \\ &+ \frac{1}{M_{NR}} \left(k_1 \text{Tr}(24_F^2) \text{Tr}(24_H^2) + k_2 [\text{Tr}(24_F 24_H)]^2 \right) \\ &+ \frac{1}{M_{NR}} \left(k_3 \text{Tr}(24_F^2 24_H^2) + k_4 \text{Tr}(24_F 24_H 24_F 24_H) \right). \end{aligned} \quad (38)$$

Whereas all the four kinds of non-standard fermion masses such as the singlet, the leptoquarks, the weak triplet, and the colour octet fermion specified in eq.(34) were needed to be lighter than GUT scale in [74], we need only the fermion triplet Σ and the colour octet fermion C_F to be lighter. Therefore, compared to [74] we need to fine tune relatively less number of parameters. For the mass scale in the non-renormalisable term, we use $M_{NR} \simeq$ string scale $= M_{String} \sim 10^{17}$ GeV (or reduced Planck scale $\simeq 10^{18}$ GeV). When the Yukawa couplings are switched off, all component masses in 24_F are near the GUT scale with degenerate masses $= M_F$. When SU(5) is broken by the VEV given in eq.(36) with $V_U \sim M_{GUT}$, masses of $\Sigma(3, 0, 1)$ and $C_F(1, 0, 8)$ are

$$\begin{aligned} M_\Sigma &= M_F - \frac{3Y_{24}V_U}{\sqrt{30}} + \frac{V_U^2}{M_{NR}} \left(k_1 + \frac{3}{10}(k_3 + k_4) \right), \\ M_{C_F} &= M_F + \frac{2Y_{24}V_U}{\sqrt{30}} + \frac{V_U^2}{M_{NR}} \left(k_1 + \frac{2}{15}(k_3 + k_4) \right) \end{aligned} \quad (39)$$

Other components in 24_F can be also expressed in a similar fashion as discussed in the Appendix. As we discuss below, our RG constraints on gauge coupling unification need Σ whose masses can be in the range $M_\Sigma \sim \mathcal{O}(500 - 3000)$ GeV, and correspondingly $M_{C_F} \sim \mathcal{O}(10^8 - 10^9)$ GeV compared to GUT scale values of $M_F \sim V_U \sim 10^{16}$ GeV. Then with appropriate fine tuning of parameters, the two relations in eq.(39) can give these desired masses when

$$\begin{aligned} k_3 + k_4 &\sim 0, \\ M_F - \frac{3Y_{24}V_U}{\sqrt{30}} + \frac{V_U^2}{M_{NR}} k_1 &\sim 0, \end{aligned} \quad (40)$$

$$M_{C_F} = \frac{5Y_{24}V_U}{\sqrt{30}} \quad (41)$$

for $Y_{24} \sim 10^{-7} - 10^{-5}$. When these relations are used, all component masses become superheavy except Σ and C_F as discussed in more detail in the Appendix in Sec.10.1.

4. Gauge coupling unification

4.1. Unification with lighter fermions and scalars

As discussed above, for successful unification with Δ_1, Δ_2 at two different heavy mass scales, the weak fermion triplet $\Sigma(3, 0, 1)$ and the colour octet fermion $C_F(1, 0, 8)$ are necessary. The mass hierarchy of different fields contributing to gauge coupling unification is arranged in the following order

$$M_U \geq M_{\Delta_1} (= M_{15_{H_1}}) \gg M_{\Delta_2} \gg M_{C_F} \gg M_\Sigma \gg M_W,$$

We use the standard renormalization group equations (RGEs) for the evolution of gauge couplings [78–82] and the analytic solutions are

$$\begin{aligned} \frac{1}{\alpha_i(M_Z)} &= \frac{1}{\alpha_i(M_U)} + \frac{a_i^{(1)}}{2\pi} \ln\left(\frac{M_\Sigma}{M_Z}\right) + \frac{a_i^{(2)}}{2\pi} \ln\left(\frac{M_{C_F}}{M_\Sigma}\right) + \frac{a_i^{(3)}}{2\pi} \ln\left(\frac{M_{\Delta_2}}{M_{C_F}}\right) \\ &+ \frac{a_i^{(4)}}{2\pi} \ln\left(\frac{M_{\Delta_1}}{M_{\Delta_2}}\right) + \frac{a_i^{(5)}}{2\pi} \ln\left(\frac{M_U}{M_{\Delta_1}}\right) \\ &+ \Theta_i^{(1)} + \Theta_i^{(2)} + \Theta_i^{(3)} + \Theta_i^{(4)} + \Theta_i^{(5)}, \quad (i = Y, 2L, 3C), \end{aligned} \quad (42)$$

In fact unification is at first realized [27] without $\Delta_1 \subset 15_{H1}$ which is then superimposed along with all other components of 15_{H1} upon the RG evolution pattern with $M_{\Delta_1} = M_{15_{H1}} \geq 10M_{\Delta_2}$. Precision gauge coupling unification is found to be left unaltered by such superimposition except for changing the value of α_G^{-1} by $\leq 5\%$ [28, 56, 57]. The one-loop and two-loop coefficients in their respective ranges of mass scales are presented in Table 5. The terms $\Theta_i^{(k)}$, ($k = 1, 2, \dots, 5$) are the two-loop contributions in the respective ranges of mass scales in this unification model. Defining the four two-loop to one-loop beta function coefficient ratios

$$B_{ij}^{(k)} = a_{ij}^{(k)} / a_j^{(k)} \quad (k = 1, 2, 3, 4), \quad (43)$$

the $\Theta_i^{(k)}$ functions are

$$\begin{aligned} \Theta_i^{(1)} &= \frac{1}{4\pi} \sum_j B_{ij}^{(1)} \ln \frac{\alpha_j(M_\Sigma)}{\alpha_j(M_Z)}, \quad \Theta_i^{(2)} = \frac{1}{4\pi} \sum_j B_{ij}^{(2)} \ln \frac{\alpha_j(M_{C_8})}{\alpha_j(M_\Sigma)}, \\ \Theta_i^{(3)} &= \frac{1}{4\pi} \sum_j B_{ij}^{(3)} \ln \frac{\alpha_j(M_\Delta)}{\alpha_j(M_{C_8})}, \\ \Theta_i^{(4)} &= \frac{1}{4\pi} \sum_j B_{ij}^{(4)} \ln \frac{\alpha_j(M_{\Delta_1})}{\alpha_j(M_{\Delta_2})}. \end{aligned} \quad (44)$$

As $a_2^{(5)} = 0$, $\Theta_i^{(5)}$ is determined by direct integration in the range $M_{\Delta_1} \rightarrow M_U$

$$\Theta_i^{(5)} = \frac{1}{8\pi^2} \sum_j a_{ij}^{(5)} \int_{M_{\Delta_1}}^{M_U} \alpha_j \frac{d\mu}{\mu}. \quad (45)$$

The particle content in different ranges of mass scales are summarised in Table 4. For the respective beta functions the one-loop coefficients $a_i^{(k)}$ ($k = 1, 2, \dots, 5$), and the two-loop coefficients $a_{ij}^{(k)}$ ($k = 1, 2, \dots, 5$) are given in Table 5.

Energy Scale	Particle content
$M_Z - M_\Sigma$	SMPs
$M_\Sigma - M_{C_F}$	SMPs + Σ
$M_{C_F} - M_{\Delta_2}$	SMPs + Σ + C_F
$M_{\Delta_2} - M_{\Delta_1}$	SMPs + Σ + C_F + Δ_2
$M_{\Delta_1} - M_U$	SMPs + Σ + C_F + Δ_2 + 15_{H1}

Table 4: Particle content of the model in different ranges of mass scales where SMPs stand for standard model particles.

Under the present TTM unification program through SU(5), confining for the sake of simplicity to predominantly one loop RG contributions, we have tested the model capabilities for precision gauge coupling unification for each input value of triplet fermion mass encompassing the range $M_\Sigma \simeq \mathcal{O}(500 - 3000)$ GeV consistent with neutrino oscillation data, cosmological bounds on neutrino masses and heavy scalar triplet mass predictions necessary for unflavoured or τ -flavoured leptogenesis. For this purpose we note that in Table 3 there are three distinct sets of

Mass range and k	$a_i^{(k)}$	$a_{ij}^{(k)}$
$M_Z - M_\Sigma, (k = 1)$	$\begin{pmatrix} 41/10 \\ -19/6 \\ -7 \end{pmatrix}$	$\begin{pmatrix} 199/50 & 27/10 & 44/5 \\ 9/10 & 35/6 & 12 \\ 11/10 & 9/2 & -26 \end{pmatrix}$
$M_\Sigma - M_{C_F}, (k = 2)$	$\begin{pmatrix} 41/10 \\ -11/6 \\ -7 \end{pmatrix}$	$\begin{pmatrix} 199/50 & 27/10 & 44/5 \\ 9/10 & 163/6 & 12 \\ 11/10 & 9/2 & -26 \end{pmatrix}$
$M_{C_F} - M_{\Delta_2}, (k = 3)$	$\begin{pmatrix} 41/10 \\ -11/6 \\ -5 \end{pmatrix}$	$\begin{pmatrix} 199/50 & 27/10 & 44/5 \\ 9/10 & 163/6 & 12 \\ 11/10 & 9/2 & 22 \end{pmatrix}$
$M_{\Delta_2} - M_{\Delta_1}, (k = 4)$	$\begin{pmatrix} 47/10 \\ -7/6 \\ -5 \end{pmatrix}$	$\begin{pmatrix} 83/10 & 171/10 & 44/5 \\ 57/10 & 275/6 & 12 \\ 11/10 & 9/2 & 22 \end{pmatrix}$
$M_{\Delta_1} - M_U, (k = 5)$	$\begin{pmatrix} 88/15 \\ 0 \\ -23/6 \end{pmatrix}$	$\begin{pmatrix} 641/50 & 43/2 & 44/5 \\ 21/2 & 387/6 & 12 \\ 11/10 & 9/2 & 22 \end{pmatrix}$

Table 5: One-loop and two-loop beta function coefficients in the respective ranges of mass scales.

mass-parameter combinations, $(M_{\Delta_1}, M_{\Delta_2}, \mu_{\Delta_1})$, each set leading to two solutions corresponding to NO and IO type neutrino mass hierarchies [34] depending upon two different values of the LNV coupling parameter μ_{Δ_2} .

Set-I:

$$\begin{aligned}
M_{\Delta_1} &= 3 \times 10^{12} \text{GeV}, \\
\mu_{\Delta_1} &= m_{(15H1,5H)} = 10^{12} \text{GeV}, \\
M_{\Delta_2} &= 10^{11} \text{GeV}, \\
\mu_{\Delta_2} &= m_{(15H2,5H)} = 3.6 \times 10^9 \text{GeV}, \text{ (NO)}, \\
\mu_{\Delta_2} &= m_{(15H2,5H)} = 3.2 \times 10^9 \text{GeV}, \text{ (IO)}.
\end{aligned} \tag{46}$$

Set-II:

$$\begin{aligned}
M_{\Delta_1} &= 3 \times 10^{13} \text{GeV}, \\
\mu_{\Delta_1} &= m_{(15H1,5H)} = 10^{13} \text{GeV}, \\
M_{\Delta_2} &= 10^{12} \text{GeV}, \\
\mu_{\Delta_2} &= m_{(15H2,5H)} = 2.4 \times 10^{10} \text{GeV}, \text{ (NO)}, \\
\mu_{\Delta_2} &= m_{(15H2,5H)} = 2.0 \times 10^{10} \text{GeV}, \text{ (IO)}.
\end{aligned} \tag{47}$$

Set-III:

$$\begin{aligned}
M_{\Delta_1} &= 3 \times 10^{13} \text{GeV}, \\
\mu_{\Delta_1} &= m_{(15H1,5H)} = 10^{13} \text{GeV}, \\
M_{\Delta_2} &= 5 \times 10^{12} \text{GeV}, \\
\mu_{\Delta_2} &= m_{(15H2,5H)} = 2.6 \times 10^{11} \text{GeV}, \text{ (NO)}, \\
\mu_{\Delta_2} &= m_{(15H2,5H)} = 2.1 \times 10^{11} \text{GeV}, \text{ (IO)}.
\end{aligned} \tag{48}$$

where we have identified in this work the respective LNV couplings $\mu_{\Delta_i} (i = 1, 2)$ as originating from fine tuning of respective SU(5) invariant trilinear couplings

$$\mu_{\Delta_i} = m_{(15H_i,5H)} (i = 1, 2) \subset m_{(15H_i,5H)} (15H_i.5H5H) (i = 1, 2), \tag{49}$$

as also noted through eq.(35) and discussions following eq.(37). As these trilinear coupling values do not affect running of gauge couplings, it is sufficient to prove precision gauge coupling unification of all the six different solutions of Table 3 if we prove such unification only for three different sets of scalar mass triplet combinations $(M_{\Delta_1}, M_{\Delta_2})$ given in eq.(46), eq.(47), and eq.(48). In our TTM unification program through SU(5) presented below in Table 6 and Table 7 we have designated such solutions as Sol.-I, Sol.-II, and Sol.-III each of which represents the respective pair of solutions of Table 3 and eq.(46), eq. (47), and eq.(48). To be more explicit, each of the unification solutions (Sol.-I, Sol.-II, and Sol.-III) presented in Table 6 or Table 7 has the two sets of values of trilinear couplings specified in eq.(46), eq.(47), and eq.(48) corresponding to the respective pair of solutions of Table 3 representing NO or IO type neutrino mass hierarchy. Thus every set of parametric solutions of Table 3 derived in [34] has one-to-one correspondence to our unification solutions realised in this work.

It has been theoretically concluded that the thermally produced triplet fermion Σ can act as the whole of the DM of the Universe by accounting for the entire value of the observed cosmological relic density $(\Omega h^2)_{Obs} = 0.1172 - 0.1224$ [5, 7] = $(\Omega h^2)_{\Sigma}$ if its perturbatively estimated resonance mass is $M_{\Sigma} \simeq 2.4$ TeV [61] which increases to $M_{\Sigma} \geq 2.74$ TeV when non-perturbative Sommerfeld enhancement is included [59, 64]. This non-perturbative resonance value has been also noted to be heavier, $M_{\Sigma} \simeq 3.0 - 3.2$ TeV [89], or even $M_{\Sigma} \simeq 4$ TeV [105]. All such heavier resonance masses of the fermionic triplet as dominant thermal DM are certainly accommodated by one class (designated under class (i) solutions) of our RG solutions to the present TTM unification program through SU(5)¹.

On the other hand, we have discussed in Sec. 5.0.3 and Sec. 6 a number of indirect experimental search constraints which forbid Σ to have such heavier resonance mass values. If these indirect search constraints are respected, then for lighter $M_{\Sigma} \ll 2.4$ TeV, permitted by the other class (= class (ii)) of the present RG unification solutions, Σ may act as a sub-dominant thermal DM component that can not account for the entire value of the observed relic density. In that case, for such class (ii) solutions, as we discuss below, we introduce an additional scalar singlet DM component ξ . The combined scalar and fermionic component contribution is suggested to account for the observed relic density as discussed in Sec. 6. Our RG solutions for TTM unification through SU(5) is found to accommodate both these two classes of WIMP DM solutions: (i) dominant fermionic triplet DM solutions with $M_{\Sigma} \geq 2.4$ TeV where a resonance value of M_{Σ} accounts for the observed relic density (ii) sub-dominant lighter fermionic triplet DM with $M_{\Sigma} \simeq O(500 - 2000)$ GeV permitted by indirect search constraints where the added presence of a scalar singlet DM ξ compensates for the deficit in the observed value of relic density.

Renormalisation group (RG) evolution of three inverse fine structure constants for one of these lower Σ masses under the class (ii) model solutions with $M_{\Sigma} = 500$ GeV is shown in Fig.2. We have also examined the RG evolutions of the three individual gauge couplings of the SM, $g_i(\mu)$ ($i = Y, 2L, 3C$) which have been shown in Fig. 3.

The colour octet fermion masses needed for unification are safely above the cosmologically allowed limit [83]. Our predictions of mass scales and the GUT scale gauge coupling are also presented in Table 6 as an example of class (ii) solutions for lighter Σ with $M_{\Sigma} = 500$ GeV.

Sol. Type	α_G^{-1}	M_U (GeV)	M_{C_F} (GeV)	M_{Δ_1} (GeV)	$m_{(15H1,5H)}$ (GeV)	M_{Δ_2} (GeV)	$m_{(15H2,5H)}$ (GeV)	Hierarchy
I	37.3	3.46×10^{15}	1.4×10^8	3×10^{12}	10^{12}	10^{11}	3.6×10^9	NO
	37.3	3.46×10^{15}	1.4×10^8	3×10^{12}	10^{12}	10^{11}	3.2×10^9	IO
II	37.50	3.46×10^{15}	6.3×10^8	3×10^{13}	10^{13}	10^{12}	2.4×10^{10}	NO
	37.50	3.46×10^{15}	6.3×10^8	3×10^{13}	10^{13}	10^{12}	2.0×10^{10}	IO
III	37.55	3.46×10^{15}	8×10^8	3×10^{13}	10^{13}	5×10^{12}	2.6×10^{11}	NO
	37.55	3.46×10^{15}	3×10^9	3×10^{13}	10^{13}	5×10^{12}	2.1×10^{11}	IO

Table 6: RG solutions for mass scales and GUT coupling constant in concordance with precision gauge coupling unification and scalar triplet masses fitting the neutrino oscillation data and leptogenesis in the case of the TTM embedding in non-supersymmetric SU(5) for the fermionic triplet mass $M_{\Sigma} = 500$ GeV.

It is to be noted that in Table 6, each of the solutions (I, II, and III) represents unification of a pair of corresponding solutions presented in Table 3 and as explained through eq.(46),eq.(47), eq.(48) and eq.(49). Whereas Sol.I represents

¹We have checked that similar Unification solutions are possible also with $M_{\Sigma} \simeq 4$ TeV [105] leading to $M_U \simeq O(10^{15})$ GeV.

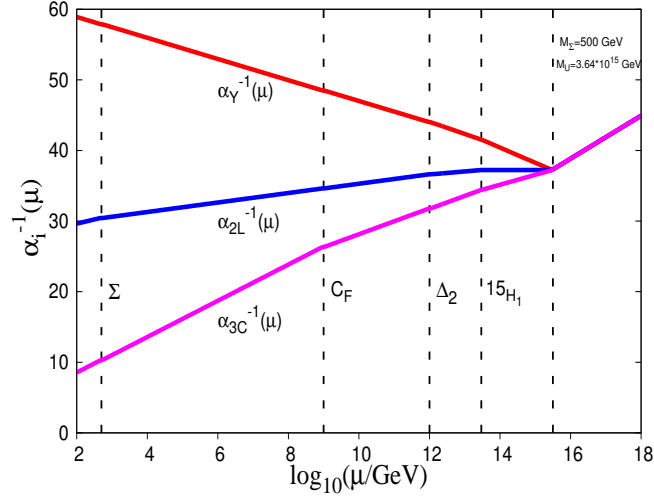


Figure 2: Unification of inverse fine structure constants of the SM gauge group $SU(3)_C \times SU(2)_L \times U(1)_Y$ at the GUT scale $M_U = 10^{15.54}$ GeV in the presence of masses of lighter scalar triplet $M_{\Delta_2} = 10^{12}$ GeV, heavier scalar triplet $M_{\Delta_1} = M_{15H_1} = 10^{13.5}$ GeV, weak triplet fermion $M_\Sigma = 500$ GeV, and colour octet fermion $M_{C_F} = 10^9$ GeV.

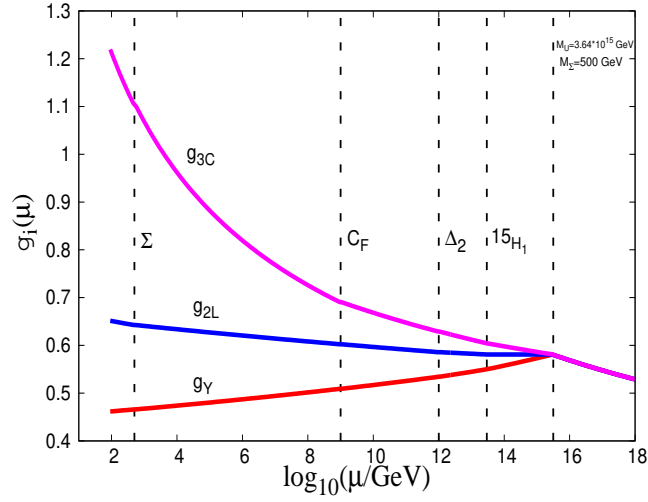


Figure 3: Renormalization group evolutions of three gauge couplings of the SM in the presence of two scalar triplets and other particles as in Fig. 2 showing precision unification at $\mu = M_U = 10^{15.54}$ GeV for $M_\Sigma = 500$ GeV.

unification of successful τ - flavoured leptogenesis, Sol.II and Sol.III represent successful unification of unflavoured leptogenesis. All the three sets of solutions are compatible with successful fits to neutrino oscillation data for both NO and IO types of mass hierarchies.

In Sec.5 we have discussed phenomenological importance of triplet fermionic DM covering the mass range $M_\Sigma = O(500 - 3000)$ GeV all of which are consistent with direct detection cross section limits measured by XENON1T [9, 10]. Out of these masses, the perturbatively estimated resonance value $M_\Sigma = 2.4$ TeV (or Sommerfeld enhancement boosted value $M_\Sigma \geq 2.74$ TeV) corresponding to dominant fermionic triplet thermal DM has been noted to account for the entire observed cosmological relic density. An example of unification solutions for such heavier Σ under class (i) solution category for $M_\Sigma = 2.4$ TeV is presented in Table 7 accommodating all the three sets of bench mark solutions of Table 3 as explained further through eq.(46), eq.(47), eq.(48), and eq.(49). Analogous to the $M_\Sigma = 500$ GeV example of class (ii) solutions applicable for lighter Σ presented in Table 6, we have thus established one-to-one correspondence of ununified solutions of Table 3 with the resonance mass $M_\Sigma = 2.4$ TeV example of our class (i) solutions.

Sol. Type	α_G^{-1}	M_U (GeV)	M_{C_F} (GeV)	M_{Δ_1} (GeV)	$m_{(15H1,5H)}$ (GeV)	M_{Δ_2} (GeV)	$m_{(15H2,5H)}$ (GeV)	Hierarchy
I	38.1	2.3×10^{15}	1.4×10^9	3×10^{12}	10^{12}	10^{11}	3.6×10^9	NO
	38.1	2.3×10^{15}	1.4×10^9	3×10^{12}	10^{12}	10^{11}	3.4×10^9	IO
II	38.3	2.3×10^{15}	2.7×10^9	3×10^{13}	2×10^{13}	10^{12}	2.4×10^{10}	NO
	38.3	2.3×10^{15}	2.7×10^9	3×10^{13}	2×10^{13}	10^{12}	2×10^{10}	IO
III	38.35	2.3×10^{15}	3×10^9	3×10^{13}	2.6×10^{11}	5×10^{12}	2.6×10^{11}	NO
	38.35	2.3×10^{15}	3×10^9	3×10^{13}	2.6×10^{11}	5×10^{12}	2.1×10^{11}	IO

Table 7: RG solutions for mass scales and GUT coupling constant in concordance with precision gauge coupling unification and scalar triplet masses fitting the neutrino oscillation data and leptogenesis in the case of the TTM embedding in non-supersymmetric SU(5) for the fermionic triplet DM perturbative resonance mass $M_\Sigma = 2.4$ TeV.

RG evolutions of the three inverse fine structure constants under class (i) solutions with $M_\Sigma = 2.4$ TeV, $M_{C_F} = 3.16 \times 10^9$ GeV, $M_{\Delta_2} = 10^{12}$ GeV, and $M_{\Delta_1} = 3 \times 10^{13}$ GeV are presented in Fig. 4 showing precision gauge coupling unification at $M_U \simeq 2.3 \times 10^{15}$ GeV. In the following Sec. 4.2 we have noted that such $\simeq 30\%$ decrease in the unification scale, compared to $M_U = 3.46 \times 10^{15}$ GeV for $M_\Sigma = 500$ GeV given in Table 6, poses no problem for proton life time compliance with Hyper-Kamiokande limit [68] in this model as the unknown mixing V_{eff} can assume correspondingly smaller values [54, 55, 73]. .

4.2. Proton lifetime estimation

The ongoing experimental search for proton decay at Hyper-Kamiokande has set the lower limits on the life time for the decay mode $p \rightarrow e^+ \pi^0$ [68]

$$\tau_p^{HypK.}(p \rightarrow e^+ \pi^0) \geq 8 \times 10^{34} \text{ yrs}, \quad (50)$$

whereas the Super-Kamiokande bound [67] is $\tau_p^{SupK.}(p \rightarrow e^+ \pi^0) \geq 1.6 \times 10^{34}$ yrs. We discuss how far the present SU(5) model is capable of respecting these bounds. Including strong and electroweak renormalisation effects on the dim.6 operator and taking into account fermion mixing[54, 55, 73], chiral symmetry breaking effects, and lattice gauge theory estimations, the decay width [84–88] is

$$\Gamma(p \rightarrow e^+ \pi^0) = \frac{\pi m_p \alpha_G^2}{2M_U^2} \times A^2 V_{eff}^2 |\mathcal{M}|^2. \quad (51)$$

In eq.(51) $m_p = 939$ MeV, $A = A_L A_S$, $A_L(A_S) =$ Long (short) distance renormalization factor which has been estimated below, and the matrix element \mathcal{M} is identified as

$$\mathcal{M} = \langle \pi^0 | (ud)_{RUL} | p \rangle, \quad (52)$$

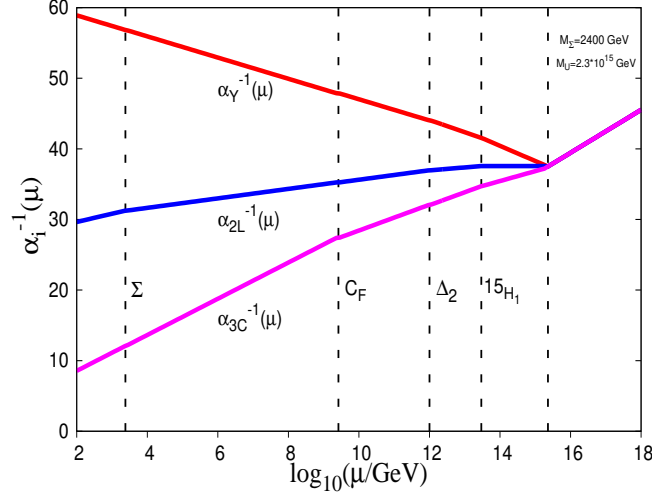


Figure 4: RG evolutions of inverse fine structure constants of the SM gauge group $SU(3)_C \times SU(2)_L \times U(1)_Y$ showing unification at the GUT scale $M_U = 2.30 \times 10^{15}$ GeV in the presence of masses of lighter scalar triplet $M_{\Delta_2} = 10^{12}$ GeV, heavier scalar triplet $M_{\Delta_1} = M_{15H_1} = 3 \times 10^{13}$ GeV, weak triplet fermion $M_\Sigma = 2.4$ TeV, and colour octet fermion $M_{C_F} = 2.68 \times 10^9$ GeV.

leading to the formula for proton lifetime is

$$\begin{aligned} \Gamma^{-1}(p \rightarrow e^+ \pi^0) &= \tau_p(p \rightarrow e^+ \pi^0) \\ &= \frac{2}{\pi m_p} \frac{M_U^4}{\alpha_G^2} \frac{1}{A^2 V_{eff}^2} \frac{1}{|\mathcal{M}|^2}. \end{aligned} \quad (53)$$

Denoting the generational mixing indices by $\alpha\beta$ in the mixing matrix $V_i^{\alpha\beta}$ ($i = 1, 2, 3$), the parameter V_{eff} is defined as [54, 55, 73]

$$V_{eff}^2 = \left(|(V_2^{11} + V_{UD}^{11}(V_2 V_{UD})^{11})|^2 + |V_3^{11}|^2 \right). \quad (54)$$

Dropping the superscripts for convenience

$$\begin{aligned} V_2 &= E_C^\dagger D, \quad V_3 = D_C^\dagger E, \\ V_3 &= D_C^\dagger E, \quad V_{UD} = U^\dagger D. \end{aligned} \quad (55)$$

Here U, E, and D matrices in eq.(55) are the diagonalising matrices of Yukawa matrices for up-quarks, charged leptons and down quarks, respectively:

$$\begin{aligned} Y_u^{diag} &= U_C^T Y_u U, \quad Y_d^{diag} = D_C^T Y_d D, \\ Y_e^{diag} &= E_C^T Y_e E. \end{aligned} \quad (56)$$

Although the elements of the CKM matrix V_{UD} are known, the mixing matrices V_2 and V_3 are unknown in such SU(5) models making the parameter V_{eff} undetermined by the model itself. For our estimation we will use a wider range of values of this parameter: $V_{eff} = 0.1 - 1.0$ [54, 55] to have an idea how far present and future measurements can constrain this model compared to similar studies in SO(10) [28]. Although in the anti-neutrino decay channels $p \rightarrow \pi^+ \bar{\nu}$ and $p \rightarrow K^+ \bar{\nu}$, it is possible to predict upper bounds on the respective lifetimes [54, 55], we plan to carry

out these separately including threshold effects which have been shown to play a significant role [27]. Using recent estimations [87, 88]

$$\mathcal{M} = \langle \pi^0 | (ud)_{RUL} | p \rangle = -0.103(23)(34) \text{GeV}^2, \quad (57)$$

$$\mathcal{M} = -.131(4)(13) \text{GeV}^2, \quad (58)$$

we will estimate τ_P for $V_{eff} = 0.1 - 1.0$ [54] and both these matrix inputs from [87, 88].

4.2.1. Long and short distance corrections for dim.6 operator

The proton lifetime formula discussed in Sec.4.2 contains short distance (A_S) and long distance (A_L) renormalisation factors. The long distance renormalisation factor A_L occurring in the proton decay width of eq.(51) and in eq.(53) of Sec.4.2) represents evolution of the dim.6 operator for mass scales $\mu = Q = 2.3 \text{ GeV}$ to $\mu = M_Z$. This factor A_L is the same for all the three models

$$A_L = \left(\frac{\alpha_3(M_b)}{\alpha_3(M_Z)} \right)^{\frac{6}{23}} \left(\frac{\alpha_3(Q)}{\alpha_3(M_b)} \right)^{\frac{6}{25}}. \quad (59)$$

Numerically we estimate its value to be

$$A_L = 1.15 \quad (60)$$

The short distance renormalisation factor is

$$\begin{aligned} A_S &= \left(\frac{\alpha_3(M_Z)}{\alpha_3(M_{\sigma_F})} \right)^{\frac{-2}{a_3^{(1)}}} \left(\frac{\alpha_3(M_{\sigma_F})}{\alpha_3(M_{C_F})} \right)^{\frac{-2}{a_3^{(2)}}} \left(\frac{\alpha_3(M_{C_F})}{\alpha_3(M_{\Delta_2})} \right)^{\frac{-2}{a_3^{(3)}}} \\ &\times \left(\frac{\alpha_3(\Delta_2)}{\alpha_3(M_{\Delta_1})} \right)^{\frac{-2}{a_3^{(4)}}} \left(\frac{\alpha_3(M_{\Delta_1})}{\alpha_3(M_U)} \right)^{\frac{-2}{a_3^{(5)}}} \\ &\times \left(\frac{\alpha_2(M_Z)}{\alpha_2(M_{\sigma_F})} \right)^{\frac{-9}{4a_2^{(1)}}} \left(\frac{\alpha_2(M_{\sigma_F})}{\alpha_2(M_{C_F})} \right)^{\frac{-9}{4a_2^{(2)}}} \left(\frac{\alpha_2(M_{C_F})}{\alpha_2(M_{\Delta_2})} \right)^{\frac{-9}{4a_2^{(3)}}} \\ &\times \left(\frac{\alpha_1(M_Z)}{\alpha_1(M_{\sigma_F})} \right)^{\frac{-11}{20a_1^{(1)}}} \left(\frac{\alpha_1(M_{\sigma_F})}{\alpha_1(M_{C_F})} \right)^{\frac{-11}{20a_1^{(2)}}} \left(\frac{\alpha_1(M_{C_F})}{\alpha_1(M_{\Delta_2})} \right)^{\frac{-11}{20a_1^{(3)}}} \\ &\times \left(\frac{\alpha_1(M_{\Delta_2})}{\alpha_1(M_{\Delta_1})} \right)^{\frac{-11}{20a_1^{(4)}}} \left(\frac{\alpha_1(M_{\Delta_1})}{\alpha_1(M_U)} \right)^{\frac{-11}{20a_1^{(5)}}}, \end{aligned} \quad (61)$$

where $M_{\Delta_1} = M_{15H_1}$. Using the one-loop beta function coefficients and coupling constant values at the respective mass scales $\mu = M_Z, M_\Sigma, M_{C_F}, M_{\Delta_2}, M_{\Delta_1}, M_U$, we have estimated

$$A_S = 2.238, A = A_S A_L = 2.576 \quad (62)$$

Using these model parameters in eq.(53), proton lifetime estimations for $M_U = 10^{15.54} \text{ GeV}$ are shown in Fig.5 for the $p \rightarrow e^+ \pi^0$ decay mode as a function of the parameter $V_{eff} = 0.1 - 1.0$. Out of different experimental bounds [67, 68], the stronger one is due to [68]. It is clear that the values of $V_{eff} \geq 2$ are ruled out by both the current limits [67, 68] unless threshold effects are taken into account. But a large region of the parameter space for $V_{eff} < 1$ is likely to remain unconstrained in near future unless the actual proton decay is detected to fix this model parameter. Future improved measurements over the current Hyper-Kamiokande limit [68] would further constrain the parameter space spanned by V_{eff} [54, 73].

Compared to $M_\Sigma = 500 \text{ GeV}$ solutions of Table 6 for which the GUT scale is $M_U = 3.46 \times 10^{15} \text{ GeV}$, our solutions for heavier fermionic triplet mass $M_\Sigma = 2.4 \text{ TeV}$ yields $M_U = 2.3 \times 10^{15} \text{ GeV}$ which is nearly 30% lighter. Proton lifetime estimations corresponding to $M_\Sigma = 2.4 \text{ TeV}$ solution are presented in the upper and lower panels of Fig.6 for lattice gauge theory matrix elements $\mathcal{M} = -0.103 \text{ GeV}^2$ and $\mathcal{M} = -0.131 \text{ GeV}^2$, respectively [87, 88]. Whereas Hyper-Kamiokande experimental limit could be satisfied with the unknown mixing parameter $V_{eff} \simeq 1$ for $M_\Sigma = 500 \text{ GeV}$ solutions, lower values of $V_{eff} = 0.4 - 0.8$ are needed for the $M_\Sigma = 2.4 \text{ TeV}$ solutions. For the values of the entire range of triplet fermion masses used as input parameter $M_\Sigma \simeq O(500 - 3000) \text{ GeV}$, while maintaining the same

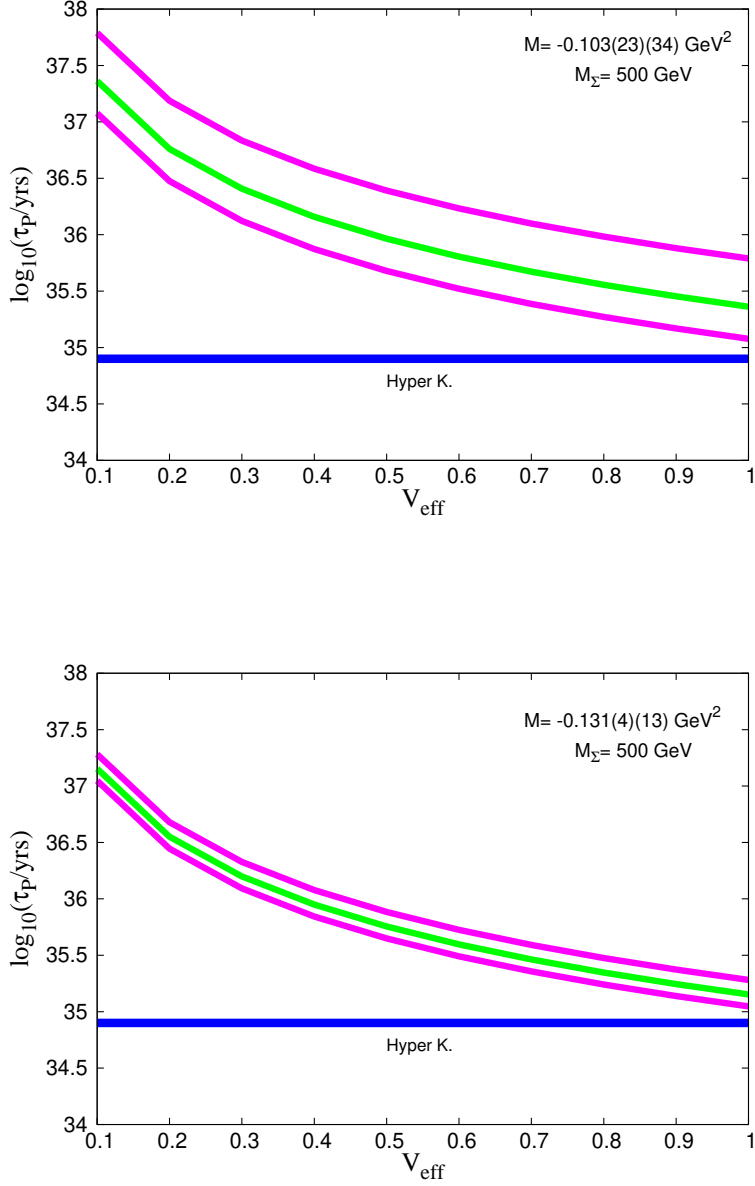


Figure 5: Proton lifetime estimation for solutions of Table 6 corresponding to $M_\Sigma = 500 \text{ GeV}$ as a function of the unknown mixing parameter V_{eff} for the decay mode $p \rightarrow e^+ \pi^0$ for two values of the matrix element (i) $M = -0.103(23)(34) \text{ GeV}^2$ (upper figure), (ii) $M = -0.131(4)(13) \text{ GeV}^2$ (lower figure). In each figure the upper and lower curves represent respective uncertainties in the matrix element [87, 88]. The horizontal lines in both the figures indicate the Hyper-Kamiokande limit [68]: $\tau_p = 8 \times 10^{34} \text{ yrs}$.

values of Δ_1 and Δ_2 masses but with variations over the corresponding values of M_{C_F} and M_U given in Table 6 and Table 7, we find precision coupling unification yielding $M_U \simeq (10^{15.53} - 10^{15.28}) \text{ GeV}$ all of which are capable of yielding proton lifetimes longer than Hyper-Kamiokande limit by suitably adjusting the mixing parameter V_{eff} . Thus the entire range of masses $M_\Sigma \simeq \mathcal{O}(500 - 3000) \text{ GeV}$ are consistent with precision gauge coupling unification in the

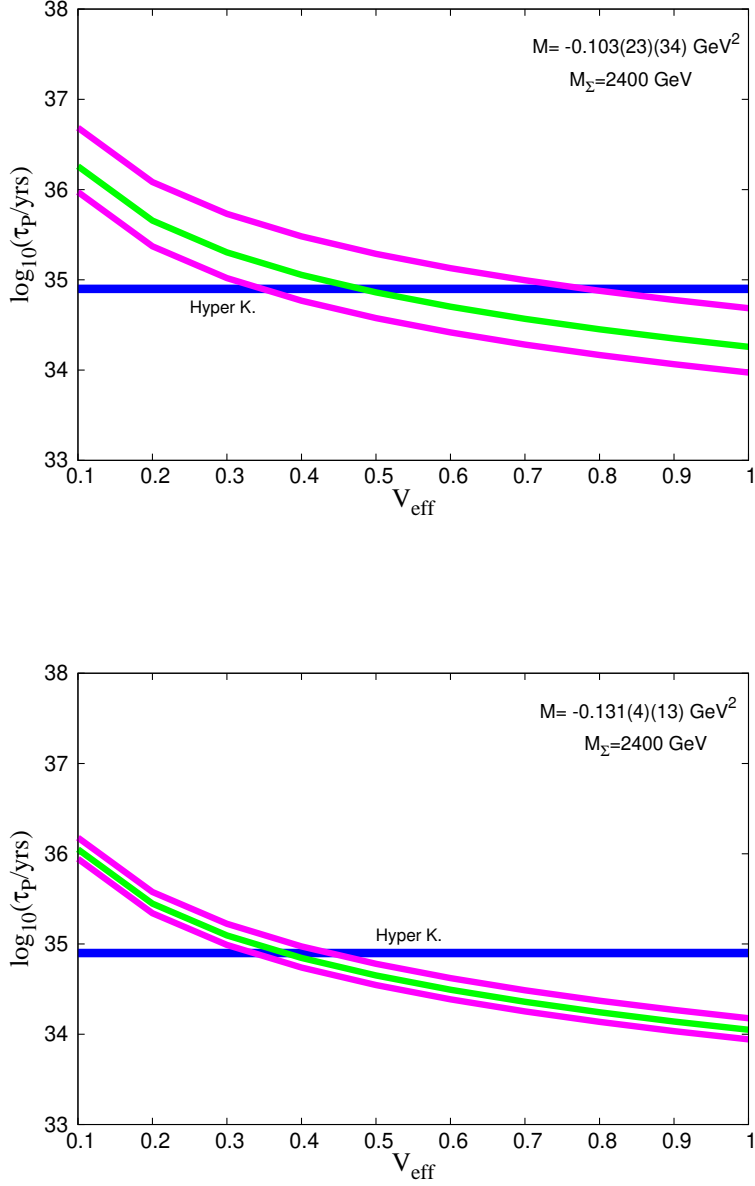


Figure 6: Proton lifetime estimation for solutions of Table 7 corresponding to $M_\Sigma = 2400 \text{ GeV}$ as a function of the unknown mixing parameter V_{eff} for the decay mode $p \rightarrow e^+\pi^0$ for two values of the matrix element (i) $M = -0.103(23)(34) \text{ GeV}^2$ (upper figure), (ii) $M = -0.131(4)(13) \text{ GeV}^2$ (lower figure). In each figure the upper and lower curves represent respective uncertainties in the matrix element [87, 88]. The horizontal lines in both the figures indicate the Hyper-Kamiokande limit [68]: $\tau_p = 8 \times 10^{34} \text{ yrs}$.

present SU(5) model predicting the same sets of values of heavy Δ_1, Δ_2 masses fitting the neutrino oscillation data and baryon asymmetry of the Universe through similar ansatz for unflavoured or partially flavoured leptogenesis.

5. Fermionic triplet dark matter

In Sec.4 we have found that the embedding of the TTM in $SU(5)$ with precision gauge coupling unification predicts a triplet fermion $\Sigma(3, 0, 1)$ and a colour octet fermion $C_F(1, 0, 8)$ both of which have been suggested to originate from the non-standard fermionic representation $24_F \subset SU(5)$. The phenomenology of a hyperchargeless triplet fermionic DM in the non-SUSY model is similar to that of the wino DM in MSSM and SUSY GUTs which has been investigated recently [59, 60, 64, 89–91, 95], and also continues to be a subject of current importance [89–91]. It is pertinent to note that if Σ represents a non-thermal DM, it can account for the entire value of the observed relic density [5, 7] for each value of its hitherto experimentally undetermined mass $M_\Sigma < 3000$ GeV [89–91], which have been found to complete precision gauge coupling unification through $SU(5)$ as noted above. The wino dominated DM cosmological relic density prediction has been also normalised to its observed value even at $M_\Sigma \simeq 100$ GeV while searching for its signature at LHC with proposed upgradation of beam luminosity [91]. However, our discussions in this work are mainly related to thermal DM.

In the present $SU(5)$ model Σ is stabilised by an additional Z_2 discrete symmetry. In Table 8 we have presented the Z_2 charges of all particles and representations of the present $SU(5)$ theory where the $Z_2 = +1$ for $24_F, \Sigma, C_F, 5_H$ but both $\bar{5}_F$ and 10_F have $Z_2 = -1$.

Table 8: Particle representations of unified two-triplet model for neutrino mass, baryon asymmetry and dark matter with respective charges under $G_{213} \times Z_2$ and $SU(5) \times Z_2$. The second and the third generation fermions not shown in this Table have identical transformation properties as those of the first generation. The scalar singlet DM ξ compensates for the relic density missed by the fermionic DM Σ constrained by indirect experimental searches and also satisfies direct detection experimental bounds discussed in Sec. 6.

Particle	G_{213}	$SU(5)$	Z_2
$(\nu, e)_L^T$	$(2, -1/2, 1)$	$\bar{5}_F$	-1
e_R	$(1, -1, 1)$	10_F	-1
$(u, d)_L^T$	$(2, 1/6, 3)$	10_F	-1
u_R	$(1, 2/3, 3)$	10_F	-1
d_R	$(1, -1/3, 3)$	$\bar{5}_F$	-1
Σ	$(3, 1, 0)$	24_F	+1
C_F	$(1, 0, 8)$	24_F	+1
ϕ	$(2, 1/2, 1)$	5_H	+1
Δ_1	$(3, -1, 1)$	15_{H1}	+1
Δ_2	$(3, -1, 1)$	15_{H2}	+1
S_{24}	$(1, 0, 1)$	24_H	+1
ξ	$(1, 0, 1)$	1_H	-1

These assignments rule out type-III seesaw mediation [74] by the fermion triplet Σ or type-I seesaw mediation by the fermion singlet $S_F(1, 0, 1) \subset 24_F$ establishing type-II seesaw as the only allowed source of neutrino mass in such two-triplet embedding through $SU(5) \times Z_2$. These Z_2 charge assignments further forbid loop mediation through vertex correction diagrams of Higgs scalar triplets bilepton decays (i.e $\Delta_{1,2} \rightarrow ll$) by the singlet or triplet components of 24_F which further establishes the hypothesis that the two triplets are rudimentary components for baryon asymmetry generation through leptogenesis.

The even value of the global discrete charge ($Z_2 = +1$) of fermion triplet DM $\Sigma(1, 3, 0) \subset 24_F$, compared to odd (even) discrete charge of standard fermion (Higgs scalar), guarantees stability of the DM by ruling out Yukawa interactions with SM fermions. Also the triplet fermion decay through discrete symmetry permitted couplings $24_F^2 24_H$ is kinematically forbidden as all other relevant masses are far more heavier than M_Σ .

5.0.1. Relic density constraints

The only interaction of the DM fermion with standard model particles is through gauge interaction that leads to the well known mass difference [59] $M_{\Sigma^\pm} - M_{\Sigma^0} = 166$ MeV where we have denoted the mass of the charged (neutral)

component of Σ as $M_{\Sigma^\pm}(M_{\Sigma^0})$.

We now discuss the implications of our unification solution $M_\Sigma \sim \mathcal{O}(1)$ TeV as WIMP dark matter [59, 60, 62, 89, 90]. Defining $\Gamma(H)$ as the particle decay rate (Hubble parameter), at a certain stage of evolution of the Universe a particle species is said to be coupled if $\Gamma > H$ or decoupled if $\Gamma < H$. The WIMP DM particle has been decoupled from the thermal bath at some early epoch and has remained as a thermal relic. For estimation of DM relic density [59–61] the corresponding Boltzmann equation [92–95] is solved approximately

$$\frac{dn}{dt} + 3Hn = -\langle\sigma v\rangle(n^2 - n_{eq}^2), \quad (63)$$

where n = actual number density at a certain instant of time (denoted as t in eq.(63)), n_{eq} = equilibrium number density of DM particle, v = velocity, and $\langle\sigma v\rangle$ = thermally averaged annihilation cross section. Approximate solution of Boltzmann equation gives the expression of relic density

$$\langle\Omega h^2\rangle_\Sigma = \frac{1.07 \times 10^9 x_F^\Sigma}{\sqrt{g_*} M_{pl} \langle\sigma_{eff}^\Sigma |v|\rangle}, \quad (64)$$

where $x_F^\Sigma = M_\Sigma/T_F$, T_F = freezeout temperature, g_* = effective number of massless degrees of freedom and $M_{pl} = 1.22 \times 10^{19}$ GeV, and the subscript or superscript indicate respective quantities associated with the fermion triplet DM $\Sigma(3, 0, 1) \equiv \Sigma$. The value of x_F^Σ is computed through iterative solution of the equation

$$x_F^\Sigma = \ln \left[\frac{1}{2\pi^3} \sqrt{\frac{45}{2}} \frac{M_{pl} M_\Sigma \langle\sigma_{eff}^\Sigma |v|\rangle}{\sqrt{g_* x_F^\Sigma}} \right]. \quad (65)$$

The relic abundance of the neutral component Σ^0 is theoretically estimated by taking into account the annihilations and co-annihilations of Σ^0 itself and $\Sigma^+\Sigma^-$. All such relevant cross sections, $\sigma(\Sigma^0, \Sigma^0)$, $\sigma(\Sigma^0, \Sigma^\pm)$, $\sigma(\Sigma^+, \Sigma^-)$, and $\sigma(\Sigma^\pm, \Sigma^\pm)$ are computed. Adding them up with respective weightage factors [61] gives the effective cross section $\langle\sigma_{eff}^\Sigma |v|\rangle$ which occurs in eq.(64) and eq.(65). This effective cross section is used in the right-hand side of eq.(65) while solving it iteratively to determine x_F^Σ as discussed above.

Neglecting mass difference between Σ^\pm and Σ^0 , it has been shown from perturbative estimation that [59, 60, 64]

$$\langle\sigma^\Sigma |v|\rangle = \frac{37g_{2L}^4}{96\pi M_\Sigma^2} \quad (66)$$

The correct amount of relic abundance $\Omega h^2 = 0.1172 - 0.1224$ [5, 7], is generated for $M_\Sigma \sim 2.4$ TeV [61]. This mass value emerges from perturbative estimations of annihilation and co-annihilation cross sections. However, when non-perturbative contributions with Sommerfeld enhancement effect are included, matching the relic density within 3σ uncertainty of relic density ($\Omega h^2 = 0.095 - 0.125$) needs $M_\Sigma \sim 2.75 \pm 0.15$ TeV [59, 60, 64, 95]. Heavier masses $M_\Sigma = 3.0 - 3.2$ TeV [89, 90] and $M_\Sigma \simeq 4$ TeV [105] have been also suggested. Even though Σ with a sub-dominant thermal DM mass $M_\Sigma < 3$ TeV below the Sommerfeld enhanced resonance value [89, 90] can not account for the observed cosmological relic density, it can succeed in doing so if it is non-thermal [89–91].

5.0.2. Direct detection and collider searches

(a). Direct detection prospects

In general for elastic scattering of a DM particle (which is electrically neutral) off nucleons, either a standard Higgs or a Z-boson exchange is needed in the t-channel of the dominant tree diagrams. In the absence of such couplings of Σ^0 , a sub-dominant process occurs by the exchange of two virtual W^\pm bosons through a box diagram [59]. This process leads to suppression of spin independent cross section by 2 – 3 orders below the experimentally detectable value. However, such predicted cross sections are measurable with improvement of detector sensitivities [9, 10]. Currently XENON1T collaboration [10] has measured the lowest value of this cross section up to 4.1×10^{-47} cm² which, however, has been reached only for a lower value of DM mass $M_{DM} = 30$ GeV. For heavier DM masses the measured value of direct detection cross section increases.

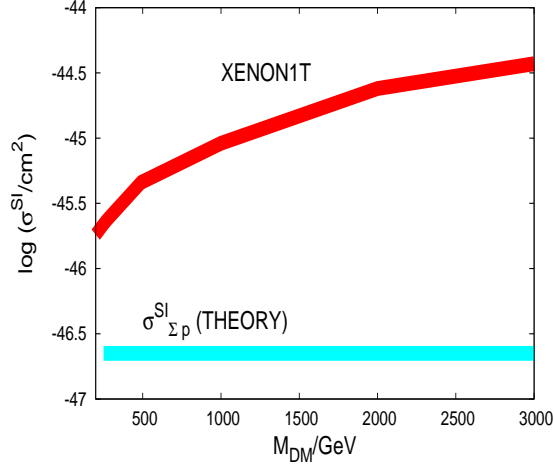


Figure 7: Comparison of experimentally determined direct detection cross section bounds on spin-independent (SI) DM-Nucleon elastic scattering from XENON1T Collaboration [9, 10] presented as red curve with theoretical predictions [96] for Σp elastic scattering denoted as green curve in the triplet fermionic DM mass range $M_\Sigma = (270 - 3000)$ GeV as discussed in the text.

The inelastic scattering off nucleons with a charged component (Σ^+ or Σ^-) is prevented because of kinematic constraints since the mass difference, $m_{\Sigma^+} - m_{\Sigma^0} = 166$ MeV, is about three orders of magnitude above the kinetic energy of Σ and also much above the proton-neutron mass difference, $m_n - m_p \sim 2$ MeV.

Theoretically, for $M_\Sigma = (270 - 3000)$ GeV, the spin independent Σp elastic scattering cross section has been recently estimated for wino DM in SUSY (with decoupled superpartners) and also in non-SUSY SM extension with Σ as a minimal DM candidate including QCD effects through two-loop contributions leading to similar results in both cases [96]

$$\sigma^{SI}(\Sigma p \rightarrow \Sigma p) \simeq (2.3_{-3.4}^{+2.5}) \times 10^{-47} \text{ cm}^2 \quad (67)$$

Here the underlying uncertainty due to perturbation theory (input parameters) has been represented by the second (third) term in the right-hand side of eq.(67). An interesting new point of this theoretical prediction is that the estimated cross section is clearly above the neutrino background [97] which makes the future direct detection prospects for Σ more promising. In Fig.7 we have compared the theoretical prediction of eq.(67) (presented as green curve) with the experimentally determined direct detection cross section bounds from XENON1T Collaboration [9, 10] in the same DM mass range $M_\Sigma = 270 - 3000$ GeV (presented as red curve). Direct detection bounds from LUX-2016 [8] and Panda X-II [11] (not shown in Fig. 7) are either larger or equal to XENON1T [9, 10] data presented by the red curve. As shown in Fig. 7, the experimentally measured direct detection cross sections increase by 1 – 3 orders beyond the theoretical prediction in the triplet fermionic DM mass range $M_\Sigma = \mathcal{O}(500 - 3000)$ GeV [96].

It is clear that for the mass range $M_\Sigma \sim 2 - 3$ TeV, the spin independent theoretical cross section due to $\Sigma - p$ elastic scattering is about $\mathcal{O}(10^{-2} - 10^{-3})$ times smaller than the current XENON1T [9, 10] and other direct detection experimental bounds from LUX-2016 [8] and Panda X-II [11] whose measured cross sections are larger than the XENON1T collaboration [10]. But Fig.7 also indicates near future possibility of direct experimental detection provided the fermionic triplet DM is in the lower mass region $270 \leq M_\Sigma/\text{GeV} < 1000$ for which accuracies of XENON1T cross section measurements have to be improved by 1-2 orders.

(b). Collider signature

Prospects of observing signatures of the triplet fermion DM at colliders have been investigated in [63, 90, 91, 98–100]. For $M_\Sigma \sim 2.7$ TeV and integrated luminosity of 100fb^{-1} , the DM pair production cross section at LHC in the channel

$pp \rightarrow \Sigma\Sigma X$ has been shown to result in only one event [63, 98, 99]. For better detection capabilities, upgradation of LHC with twice the current energy and more luminosity has been suggested [100].

Besides ref.[99, 100], collider signatures in models where Σ mediates type-III seesaw mechanism (which is ruled out in this work by Z_2 charge assignments) have been also discussed earlier [74, 101] and more recently in [102].

For detection at e^+e^- collider that requires a collision energy of at least twice the DM mass, observation of $\Sigma^+\Sigma^-$ pair production is predicted via Z boson exchange [59, 63]. The neutral pair $\Sigma^0\Sigma^{0*}$ can be also produced at LHC (or e^+e^- collider), although at a suppressed rate, through one-loop box diagram mediated by two virtual W bosons. After production, such charged components would provide a clean signal as they would manifest in long lived charged tracks due to their decays via standard gauge boson interactions, $\Sigma^\pm \rightarrow W^\pm \rightarrow \Sigma^0\pi^\pm$, or $\Sigma^\pm \rightarrow W^\pm \rightarrow \Sigma^0 l^\pm \nu_l (l = e, \mu)$. The production of e^\pm and μ^\pm charged leptons but the absence of τ^\pm due to kinematical constraint may be another distinguishing experimental signature of the triplet fermionic DM at LHC. The decay length of associated displaced vertices is clearly predicted [59, 63] to be $L_{\Sigma^\pm} \simeq 5.5$ cm.

It has been also noted in the context of $SO(10)$ [64] that the decay product Σ^0 is stable because of its matter parity which survives the GUT breaking as a gauged discrete symmetry. As such the production of this neutral component of the triplet fermion DM originating from $SO(10)$ will be signalled through missing energy [64]. This stability feature of Σ^0 with its TeV scale mass has negligible impact on electroweak precision variables. These interesting features are applicable also in the present model where the assumed Z_2 symmetry executes a role analogous to matter parity [64] in $SO(10)$.

LHC at 14 TeV energy and luminosity 1000 fb^{-1} has been shown to be capable of probing wino DM up to $M_\Sigma \simeq 600$ GeV through vector boson fusion process where the DM (\equiv non-thermal) relic density has been normalised to its observed value at as low a mass as $M_\Sigma \simeq 100$ GeV [91]. Detection possibility of Σ in the multi TeV range at high luminosity LHC and future 100 TeV pp collider has been also investigated [90] in different channels such as: (i) monojet, (ii) monophoton, (iii) vector boson (VB) fusion, and (iv) disappearing tracks. At 100 TeV, the disappearing track channels are likely to probe the resonance mass $M_\Sigma = 3$ TeV, deduced including higher order corrections and Sommerfeld enhancement, which is relevant for thermally produced DM that accounts for whole of observed relic density [89]. Although Σ as sub-dominant thermal DM can not account for observed values of relic density for lighter masses, it has been noted that it can do so for every value of the mass $M_\Sigma < 3$ TeV if it is non-thermal [89–91] whereas the relic density at $M_\Sigma \simeq 3 - 3.2$ TeV can be realised as thermal DM through Sommerfeld boosted annihilation cross section derived including higher order contributions [89]. Searches in other channels have been found to extend upto $M_\Sigma = 1.3(1.7)$ TeV for $3(30) \text{ ab}^{-1}$ of integrated luminosity provided systematics are under control [90]. These masses being away from resonance values, although a thermal Σ can not account for the entire value of observed relic density, it can do so as a non-thermal DM. For $M_\Sigma > 3.2$ TeV the DM Σ can not be treated to be thermally produced as in that case it overcloses the Universe. For such heavy masses nonthermal origin of Σ is preferred [89].

5.0.3. Prospects from indirect searches

PAMELA [103] and FERMI/LAT [104] experiments have measured the positron excess akin to wino DM model which is again confirmed by recent AMS-02 [106] data. The electron and positron fluxes are still significant in the measurement of FERMI/LAT [104]. There are various constraints on the wino dark matter from different search channels such as antiprotons, leptons, dark matter halo from diffuse galactic gamma rays, high latitude gamma-ray spectra, galaxy clusters, dwarf spheroids, gamma-ray line feature, neutrinos from the galactic halo, CMB constraints, and antideuterons [89]. In the case of the antiproton search channel, the wino dark matter having mass close to the perturbatively estimated resonance value i.e, $M_\Sigma \simeq 2.4$ TeV, and thin zone of diffusion is consistent with the antiproton measurement. But such a wino dark matter having mass near the resonance, produces very small amount of leptons and large amount of positrons at very low energy scale. This DM can not solve cosmic ray (CR) lepton puzzle because the lepton data can rule out the very proximity of resonance. The galactic γ rays also impose a stringent limit on the wino DM model. With the inclusion of the γ ray constraint, the limit on the wino DM mass changes. If the mass of DM is $M_\Sigma \sim 2.5$ TeV and it is in a thin diffusion zone, then it is excluded by the γ ray data for a wide variation of galactic cosmic ray propagation. There is also a very significant limit on the wino dark matter mass from high latitude γ ray spectra. For a 2.5 TeV wino DM, the expected 10 year cross section is $1.5 \times 10^{-25} \text{ cm}^3 \text{ s}^{-1}$ including

DM substructures [89]. Possible signatures of DM annihilations are given from γ ray observations [107, 108] towards nearby galaxy clusters but observations in ref. [109–114] have not seen any significant limits from γ ray excess. The wino dark matter having mass $M_\Sigma \simeq 2.4$ TeV can be ruled out in this search channel whereas all the other masses are allowed in the dwarf spheroids channel [89]. The winos with masses heavier than 2 TeV are excluded by the HESS [109] data at 95% CL. A new method to search for the indirect signals of DM annihilation is obtained due to the motion of high energy neutrons towards the galactic center. Wino model signals corresponding to $M_\Sigma \simeq 2.4$ TeV can be observed in this search channel [89]. There is also a constraint on the wino dark matter due to the CMB temperature and polarization power spectra. Taking WMAP-5 [115] data and with 98% CL, the DM masses in the region 2.3 TeV to 2.4 TeV have been excluded. Similarly WMAP-9 [116] excludes the region 2.25 – 2.46 TeV. But the combined search of WMAP-9 with ACT [117, 118] excludes the mass range of 2.18 – 2.5 TeV. To search for the dark matter, the most effective channel is through antideuterons. Due to the smaller signal to background ratio at mass 2.5 TeV, the resultant signal is very low with high uncertainty. With the theoretical and experimental progress, there may be stringent limit on the wino dark matter [89].

In the indirect detection experiment, signals are produced in the annihilation process: $DM DM \rightarrow SM$ particles. Here we have tree level annihilation only to W^+W^- channel. The annihilation cross section to W^+W^- shows a peak near $M_\Sigma \sim 2.7$ TeV when non-perturbative effect due to Sommerfeld enhancement is taken into account. But this high value of annihilation cross section exceeds the upper limit given by the combined analysis of Fermi/LAT [104] and MAGIC [110]. Thus when the WIMP dark matter is composed of only Σ^0 , it may be somewhat difficult to satisfy all the constraints from relic density, and direct and indirect detection experiments, simultaneously. A better agreement with PAMELA [103] positron and antiproton fluxes, and the observed cosmological relic density [7] has been suggested for a heavier wino DM of mass $M_\Sigma \simeq 4$ TeV [105] in which case precision gauge coupling unification in the present approach is possible.

Despite the constraints discussed above, the triplet fermion as a minimal, dominant thermal DM appears to be an attractive idea which is also predicted by the present unification framework. One class (= class (i)) of our solutions discussed in Sec. 3) of this SU(5) unification program with vacuum stability of the scalar potential ensured by intermediate mass scalar singlet threshold effect (as discussed below) supports Σ as dominant thermal DM of the Universe with $M_\Sigma \simeq 2.4$ TeV, or heavier [59, 60, 64, 90, 96, 105].

5.0.4. Vacuum stability

It is well known that the Higgs quartic coupling λ_ϕ of the SM scalar potential

$$V_{std} = -\mu_\phi^2 \phi^\dagger \phi + \lambda_\phi (\phi^\dagger \phi)^2, \quad (68)$$

runs negative [66] for SM Higgs field values $|\phi| \sim \mathcal{O}(10^9 - 10^{10})$ GeV causing instability to the SM vacuum that is associated with the Higgs mass $m_\phi \simeq 125$ GeV. In the renormalisation group (RG) predictions discussed in Sec.3 the TTM unification has permitted a variety of solutions for neutrino mass and leptogenesis some of which do not have this problem because of the allowed mass scale of the triplets which have threshold corrections on the quartic coupling [34]

$$\begin{aligned} \Delta\lambda_\phi^{(2)} &= \frac{\mu_2^2}{M_{\Delta_2}^2} \Theta(|\phi| - M_{\Delta_2}), \\ \Delta\lambda_\phi^{(1)} &= \frac{\mu_1^2}{M_{\Delta_1}^2} \Theta(|\phi| - M_{\Delta_1}). \end{aligned} \quad (69)$$

where $\Theta(x) = \text{Heaviside function}$. Even if the effect due to heavier Δ_1 is neglected, positive corrections due to lighter Δ_2 removes vacuum instability if $M_{\Delta_2} \simeq \mathcal{O}(10^{10})$ GeV [34]. In fact we have a class of solutions belonging to partially flavoured or τ - flavoured leptogenesis which does have such intermediate mass solutions for M_{Δ_2} in which case the model does not have vacuum instability problem.

However there is the possibility of a new class of RG solutions for unflavoured leptogenesis with much heavier triplet masses, e.g $M_{\Delta_2} \sim 10^{14}$ GeV and $M_{\Delta_1} = M_{15H_1} \sim M_U$, which does have the vacuum instability in the absence of any non-standard scalar field near $\sim \mathcal{O}10^{10}$ GeV [66] or near the electroweak scale [119, 120] in the TTM.

We note that the present SU(5) model with fine tuning in the GUT scale Higgs potential can remove such negativity of the quartic coupling for all values of $|\phi| \geq 5 \times 10^9$ GeV even if $\Delta_i (i = 1, 2)$ threshold effects in eq.(69) are negligible. This advantage occurs in this GUT framework that permits the scalar singlet $S_{24} \subset 24_H$ to be at the desired intermediate scale. The Higgs portal quartic coupling of this singlet with SM Higgs $\phi \subset 5_H$ originates from the term

$$\begin{aligned} V_q &= \lambda_S 24_H^4 + \lambda_{(\phi,S)} 24_H^2 5_H^\dagger 5_H \\ &\supset \lambda_S S_{24}^4 + \lambda_{(\phi,S)} \phi^\dagger \phi S_{24}^2. \end{aligned} \quad (70)$$

Even though $\langle S_{24} \rangle \sim M_U$, it is possible to make the SM scalar singlet mass lighter $M_{S_{24}} \simeq (10^8 - 10^9)$ GeV and this gives rise to threshold effect [66]

$$\Delta\lambda_\phi^{(S)} = \frac{\lambda_{(\phi,S)}^2}{\lambda_S} \Theta(|\phi| - M_{S_{24}}), \quad (71)$$

where λ_S = the singlet Higgs self coupling originating from $\lambda_{24} 24_H^4 \supset \lambda_S S_{24}^4$. The solution to vacuum stability issue then proceeds by RG running the SM Higgs quartic coupling and taking into account this threshold effect at the field value $|\phi| \simeq M_{S_{24}} \sim \mathcal{O}(10^8 - 10^9)$ GeV in a manner exactly similar to our earlier work [34] which we do not repeat here [28]. Thus, irrespective of the heavier mass scales $M_{\Delta_1} \gg M_{\Delta_2} \gg M_{S_{24}}$, the presence of the intermediate mass scalar singlet S_{24} at $M_{S_{24}} \sim (10^8 - 10^9)$ GeV ensures stability of the standard Higgs potential in this SU(5) theory. It is interesting to note that such a vacuum stability is maintained in the presence of both lighter (under class (ii)) and heavier triplet fermion DM mass (under class (i)) solutions contained in the mass range $M_\Sigma \sim (500 - 3000)$ GeV. In what follows, we show how this solution to vacuum stability reduces the scalar singlet DM mass prediction.

6. Fermion triplet plus scalar singlet dark matter under indirect search constraints

As discussed above the DM annihilation cross section $\Sigma^+ \Sigma^- \rightarrow W^+ W^-$ in the perturbative estimation [61] shows a peak that is capable of accounting for the cosmologically observed relic density $(\Omega h^2)_{Obs} = 0.1172 - 0.1224$ if the thermally produced triplet fermion DM mass $M_{\Sigma^0} \simeq 2.4$ TeV. However a number of indirect experimental search constraints discussed in Sec.5.0.3 forbid the Σ mass at this resonant value. For example, this dominant thermal DM mass $M_\Sigma = 2.4$ TeV does not solve the cosmic ray (CR) lepton puzzle [89] or produces excess of γ ray towards nearby galaxy clusters [107–114]. The resonance DM mass $M_\Sigma = 2.4$ TeV can be ruled out in this search channel while all other masses are allowed in the dwarf spheroids channel [89]. All mass values $M_\Sigma \geq 2$ TeV are ruled out by the HESS data [109]. Whereas the data from WMAP-5[115] have ruled out the mass range $M_\Sigma = 2.3 - 2.4$ TeV, the mass range $M_\Sigma = 2.25 - 2.46$ TeV has been ruled out by WMAP-9[116], and the combined search of WMAP-9 and ACT [117, 118] has also ruled out the mass range $M_\Sigma = 2.18 - 2.5$ TeV. Similarly the peak value of DM mass $M_\Sigma \geq 2.74$ TeV or heavier, determined through non-perturbative Sommerfeld enhancement [59, 64], appears to be ruled out as it predicts annihilation cross section exceeding the upper limit set by the combined analysis of Fermi/LAT [104] and MAGIC [110]. Consequently, these indirect search experiments constraining M_Σ to be significantly less than the resonance value 2.4 TeV (or less than the non-perturbatively determined peak value 2.74 – 3 TeV) deny the thermally produced triplet fermion Σ^0 to be the dominant WIMP DM of the Universe.

On the other hand, we have found that every Σ^- mass value in the range $M_\Sigma = \mathcal{O}(500 - 3000)$ GeV is capable of producing SU(5) unification of the TTM with precision coupling unification and prediction of the same sets of heavy scalar triplet masses matching the neutrino oscillation data, and leading to successful unflavoured or partially flavoured leptogenesis. Each of the Σ masses in the range $M_\Sigma = \mathcal{O}(500 - 3000)$ GeV also predicts spin-independent elastic $\Sigma - p$ scattering cross sections in concordance with direct detection bounds [9, 10, 96]. We have further pointed out that all classes of solutions in our unification model can be consistent with vacuum stability of the SM scalar potential caused by threshold effect due to an intermediate mass Higgs scalar singlet $S_{24} \subset 24_H$ of SU(5).

Thus, barring indirect experimental search constraints, if collider experiments in future finally succeed in detecting the heavier triplet fermion DM with perturbatively (non-perturbatively) predicted resonance mass $M_\Sigma = 2.4$ TeV ($M_\Sigma \geq 2.74$ TeV or still heavier), our unification solutions of the type given in Table 7, Fig. 4, and Fig. 6, belonging to class (i) category, are consistent with such Σ as the dominant thermal DM of the Universe accounting for the entire

value of the observed cosmological relic density [5, 7]. For this class of heavier triplet mass solutions in our unification model, there is no need to invoke the presence of a scalar singlet DM.

But if the future collider searches fail to detect such resonant $M_\Sigma = 2.4$ TeV, or heavier, and indirect experimental search constraints which forbid the resonant masses $M_\Sigma \simeq 2.4$ TeV (or corresponding non-perturbative values $M_\Sigma \simeq 2.74 - 3$ TeV) are accepted, it is difficult to account for the entire observed value of relic density with such lighter M_Σ values although they ensure TTM unification through SU(5). For such lighter $M_\Sigma < 2.0$ TeV values as sub-dominant dark matter, we propose to justify our unification solutions of the type presented in Table 6, Fig. 2, Fig. 3, and Fig. 5 also from dark matter point of view. In such other class of unification solutions corresponding to lighter $M_\Sigma < 2.0$ TeV values, we introduce a SU(5)-singlet scalar $\xi(1, 0, 1)$ as shown in Table 8 without affecting gauge coupling unification, neutrino mass, and leptogenesis results. We hypothesize the WIMP DM to comprise of two components: the neutral component of fermion triplet $\Sigma(3, 0, 1)$ of mass $M_\Sigma \sim \mathcal{O}(500 - 2000)$ GeV and the scalar singlet $\xi(1, 0, 1)$ whose mass is to be determined from relic density and direct detection mass bounds. The assignment of global discrete symmetry $Z_2(\xi) = -1$ as shown in Table 8 stabilises it as a scalar singlet component of WIMP DM [13, 34].

Similar two-component WIMP DM problem comprising of fermion triplet and scalar singlet has been addressed earlier [61] and very recently [28] where the DM was also constrained to satisfy vacuum stability by ensuring the SM Higgs quartic coupling to run positive till $|\phi| \simeq M_{pl} = 1.22 \times 10^{19}$ GeV through correction derived from DM portal. In the presence of ξ the SM Higgs potential is changed to

$$V = -\mu_\phi^2 \phi^\dagger \phi + \mu_\xi^2 \xi^\dagger \xi + \lambda_\phi (\phi^\dagger \phi)^2 + \lambda_\xi (\xi^\dagger \xi)^2 + 2\lambda_{\phi\xi} (\phi^\dagger \phi)(\xi^\dagger \xi). \quad (72)$$

leading to respective masses of standard Higgs ($= m_\phi$) and scalar DM ($= m_\xi$)

$$\begin{aligned} m_\xi^2 &= 2(\mu_\xi^2 + \lambda_{\phi\xi}^2 v^2), \\ m_\phi^2 &= 2\mu_\phi^2 = 2\lambda_\phi v^2. \end{aligned} \quad (73)$$

But unlike [28, 34], there are several other sources which can ensure vacuum stability in this model. Out of these the intermediate scale Higgs scalar singlet threshold effect of eq.(71), as discussed above in Sec.5.0.4, is capable of ensuring vacuum stability for all classes of solutions including the dominant heavy triplet fermionic DM case ($M_\Sigma = 2.4$ TeV, or $M_\Sigma \geq 2.74$ TeV).

This positive definite threshold correction is sufficient to ensure vacuum stability till the Planck scale even if threshold corrections due to two heavy scalar triplets Δ_1 and Δ_2 are neglected. The triplet fermion DM Σ does not contribute to renormalisable corrections to SM Higgs potential or its vacuum stability. In the class of our unification solutions with lower M_Σ values, the added scalar singlet DM ξ is now constrained by the part of observed relic density [5, 7] missed by the non-resonant M_Σ and the direct detection mass bounds [8–11]. As the vacuum stability constraint [34] is resolved by the intermediate scalar threshold effect, we discuss below how lower masses of the scalar DM ξ are predicted in this model.

6.0.1. Relic density constraint on scalar dark matter

A cosmologically disadvantageous point about the lighter M_Σ solutions is that the non-perturbative Sommerfeld enhancement is not effective at such masses. Also the perturbative estimation of annihilation cross section leads to the thermal relic abundance, $(\Omega h^2)_\Sigma$ significantly less than the experimentally observed value determined by Planck[5] and WMAP[7]. This deficit is compensated through the intervention of the scalar singlet DM component ξ . Since the scalar singlet can not have any renormalisable interaction with Σ , we can estimate the relic density for fermionic triplet ($= (\Omega h^2)_\Sigma$) and the scalar singlet ($= (\Omega h^2)_\xi$) separately, and add them up to get the total relic density

$$(\Omega h^2)_{Obs} = (\Omega h^2)_\Sigma + (\Omega h^2)_\xi. \quad (74)$$

where

$$(\Omega h^2)_{Obs} = 0.1172 - 0.1224, \quad (75)$$

is the observed value of cosmological DM relic density [5, 7]. For notational convenience, we also equivalently define the normalised relic density $R_\xi(R_\Sigma)$ for thermal DM component $\xi(\Sigma)$,

$$\begin{aligned} R_\xi &= \frac{(\Omega h^2)_\xi}{(\Omega h^2)_{Obs}}, \\ R_\Sigma &= \frac{(\Omega h^2)_\Sigma}{(\Omega h^2)_{Obs}}, \\ R_\Sigma + R_\xi &= 1, \end{aligned} \quad (76)$$

In the estimation of total relic density through eq.(74), essentially there are three parameters M_Σ, m_ξ and the $\xi - \phi$ Higgs portal coupling $\lambda_{\phi\xi}$. To estimate the relic abundance of the neutral component Σ^0 that acts as sub-dominant thermal dark matter, we use eq.(64) and the iterative solution from eq.(65) taking into account the annihilations and co-annihilations as explained in Sec. 5.

Since in the lower mass region of fermion triplet DM, $M_\Sigma = O(500 - 1000)$ GeV, the predicted value of $(\Omega h^2)_\Sigma$ is found to be much less than the experimentally observed value [5, 7] given in eq.(75), the total relic density is dominated by the scalar DM contribution in this M_Σ region leading to the constraint $(\Omega h^2)_{Obs} \simeq (\Omega h^2)_\xi$.

Approximate solution of the corresponding Boltzmann equation for the singlet scalar DM component ξ also gives the expression for relic density

$$(\Omega_{DM} h^2)_\xi = \frac{1.07 \times 10^9 x_F^\xi}{\sqrt{g_*} M_{pl} \langle \sigma^\xi v \rangle} \quad (77)$$

where $x_F^\xi = M_\xi/T_F$, T_F = freezeout temperature, g_* = effective number of massless degrees of freedom and $M_{pl} = 1.22 \times 10^{19}$ GeV. Now x_F^ξ can be computed by iteratively solving the equation

$$x_F^\xi = \ln \left(\frac{M_\xi}{2\pi^3} \sqrt{\frac{45 M_{pl}^2}{8 g_* x_F^\xi} \langle \sigma^\xi v \rangle} \right). \quad (78)$$

In eq.(77) and eq.(78), the only particle physics input is the thermally averaged annihilation cross section. The total annihilation cross section is obtained by summing over all the annihilation channels of the singlet DM which are $\xi\xi \rightarrow F\bar{F}, W^+W^-, ZZ, hh$ where F is symbolically used for all the fermions. Using the expression of total annihilation cross section[121, 122] in eq.(78) at first we compute x_F^ξ which is then used in eq.(77) to yield the relic density contribution due to ξ . As already noted above, in the estimation of the total relic density there are three free parameters: mass of the fermion triplet (M_Σ), mass of the scalar singlet (m_ξ) and the Higgs portal coupling ($\lambda_{\phi\xi}$). We have examined the outcome of this combined DM hypothesis, $\Sigma \oplus \xi$, upon the following values of M_Σ allowed by indirect search constraints: **(a)** $M_\Sigma \simeq (500 - 1000)$ GeV: where $R_\Sigma \simeq 0, R_\xi \simeq 1$ as explained below, and **(b)** $M_\Sigma \simeq 1.5$ TeV: where $R_\Sigma \simeq R_\xi = 0.5$.

(a) $M_\Sigma \simeq (500 - 1000)$ GeV:

$$\begin{aligned} (\Omega h^2)_\Sigma &\simeq 0, \\ R_\Sigma &\simeq 0, \\ R_\xi &\simeq 1.0. \end{aligned} \quad (79)$$

As the quantity $(\Omega h^2)_\Sigma \simeq 0$ for values of $M_\Sigma \simeq (500 - 1000)$ GeV, the scalar DM contribution to the relic density is required to meet the experimental constraint due to WMAP [7] and Planck [5] measurements:

$$0.1172 < (\Omega h^2)_\xi < 0.1224. \quad (80)$$

It is worth while to mention that we have varied $\lambda_{\phi\xi}$ and m_ξ over a wide range of values to get their first round of constraint from the relic density bound given above. Two free parameters involved in this computation are mass of the

DM particle m_ξ and the Higgs portal coupling $\lambda_{\phi\xi}$. The relic density has been estimated for a wide range of values of the scalar DM mass ranging from few GeVs to few TeVs while the coupling $\lambda_{\phi\xi}$ is also varied simultaneously in the range $(10^{-4} - 1)$. The parameters $(m_\xi, \lambda_{\phi\xi})$ are constrained by using the bound on the relic density reported by WMAP [7] and Planck [5] mentioned above in eq.(80). In Fig.8 through the yellow curve, we show only those combinations of $\lambda_{\phi\xi}$ and m_ξ which are capable of producing the entire value of the experimentally observed relic density. This yellow curve in Fig. 8 has been labelled as $(R_\xi = 1, R_\Sigma = 0)$.

(b) $M_\Sigma = 1500$ GeV:

Unlike the case (a) discussed above where Σ has almost negligible contribution to relic density, the fermionic subdominant DM has very significant contribution [95] to the experimentally observed value of relic density [5, 7] at $M_\Sigma \approx 1.5$ TeV. At first we estimate $(\Omega h^2)_\Sigma$ at $M_\Sigma = 1500$ GeV using the procedure outlines in Sec.5 and [95] leading to

$$\begin{aligned} (\Omega h^2)_\Sigma &\simeq \frac{1}{2}(\Omega h^2)_{Obs}, \\ R_\Sigma &\simeq \frac{1}{2}. \end{aligned} \quad (81)$$

Then using eq.(74) and eq.(76) gives

$$\begin{aligned} (\Omega h^2)_\xi &\simeq \frac{1}{2}(\Omega h^2)_{Obs}, \\ R_\xi &\simeq \frac{1}{2}. \end{aligned} \quad (82)$$

Following the similar procedure explained in the case (a) above, we have plotted $\lambda_{\phi,\xi}$ against m_ξ while keeping the value $R_\xi \approx 0.5$ throughout. In Fig. 8 these results have been presented by the blue curve labelled as $(R_\xi = R_\Sigma = 1/2)$.

6.0.2. Bounds from direct detection experiments

We have explicitly shown in Sec. 5.0.2 and Fig. 7 that for all values of fermionic triplet masses $M_\Sigma = (500 - 3000)$ GeV, the respective spin-independent (SI) $\Sigma - p$ elastic cross sections are well below the direct detection bounds due to XENON1T collaboration[9, 10]. With the set of values of $(\lambda_{\phi\xi}, m_\xi)$ already restricted by relic density bound, we proceed further to constrain them by direct detection bound applied to $\xi - N$ elastic scattering. For this two component dark matter, the constraint relation appears as [61, 123]

$$\frac{\epsilon_\Sigma}{M_\Sigma} \sigma_{\Sigma N} + \frac{\epsilon_\xi}{m_\xi} \sigma_{\xi N} < \frac{\sigma_0}{m_0}, \quad (83)$$

where the symbols have the following meanings: σ_0, m_0 are SI DM-nucleon scattering cross section and mass of the dark matter, respectively, for single component dark matter scenario. For the two component dark matter scenario under consideration $\sigma_{\Sigma N}(\sigma_{\xi N})$ is the SI scattering cross section of $\Sigma(\xi)$ with detector nucleon and $M_\Sigma(m_\xi)$ is its mass. The factor ϵ_i designates the fraction of density of the i th dark matter particle in a certain model: $\epsilon_i = \rho_i/\rho_0$ which can also be expressed in terms of thermally averaged annihilation cross sections as

$$\begin{aligned} \epsilon_\Sigma &= \frac{\langle\sigma v\rangle_\xi}{\langle\sigma v\rangle_\xi + \langle\sigma v\rangle_\Sigma} \\ \epsilon_\xi &= \frac{\langle\sigma v\rangle_\Sigma}{\langle\sigma v\rangle_\xi + \langle\sigma v\rangle_\Sigma}. \end{aligned} \quad (84)$$

Noting that $\epsilon_\Sigma \leq 1$ and $\epsilon_\xi \leq 1$, in the parameter space permitted by indirect experimental searches restricting $M_\Sigma \approx \mathcal{O}(500 - 2000)$ GeV, it is easy to verify that the inequality given by eq.(83) is satisfied.

We get exclusion plots of DM-nucleon scattering cross section and DM mass from different direct detection experiments [8–11]. The spin independent scattering cross section of singlet DM on nucleon is given by[124]

$$\sigma^{\text{SI}} = \frac{4f_R^2 \lambda_{\phi\xi}^2 \mu_R^2 m_N^2}{\pi m_\xi^2 m_h^4} \text{ (cm}^2\text{)} \quad (85)$$

where $m_h =$ mass of the SM Higgs (~ 125 GeV), $m_N =$ nucleon mass ~ 939 MeV, $\mu_R = (m_\xi m_N)/(m_\xi + m_N) =$ reduced DM-nucleon mass and the factor $f_R \sim 0.3$. Using eq.(85) the exclusion plots of $\sigma - m_\xi$ plane can be easily brought to $\lambda_{\phi\xi} - m_\xi$ plane. We superimpose the $\lambda_{\phi\xi} - m_\xi$ plots for different experiments [8–11] on the plot of allowed parameter space constrained by relic density bound.

Thus the parameter space ($\lambda_{\phi\xi}$ vs m_ξ) constrained by both the relic density and the direct detection experimental bounds can be obtained from Fig.8. Using complete dominance of ξ in the case (a) of the lighter values of $500 < M_\Sigma/\text{GeV} \leq 1000$ and using $R_\xi \approx 1$ we have different sets of values of $(\lambda_{\phi\xi}, m_\xi)$ while matching the observed relic density due to Planck [5] and WMAP [7]: $(\Omega h^2)_\xi \approx (\Omega h^2)_{Obs} = 0.1172 - 0.1224$ through eq.(79). This relic density matching is shown by the yellow curve in Fig.8 which has been also labelled as $(R_\xi = 1, R_\Sigma = 0)$. The green band represents exclusion plots obtained from dark matter direct detection experiments, LUX-2016[8], XENON1T [9, 10] and Panda-XII(2017) [11]. All points below this green band are allowed by direct detection experiments.

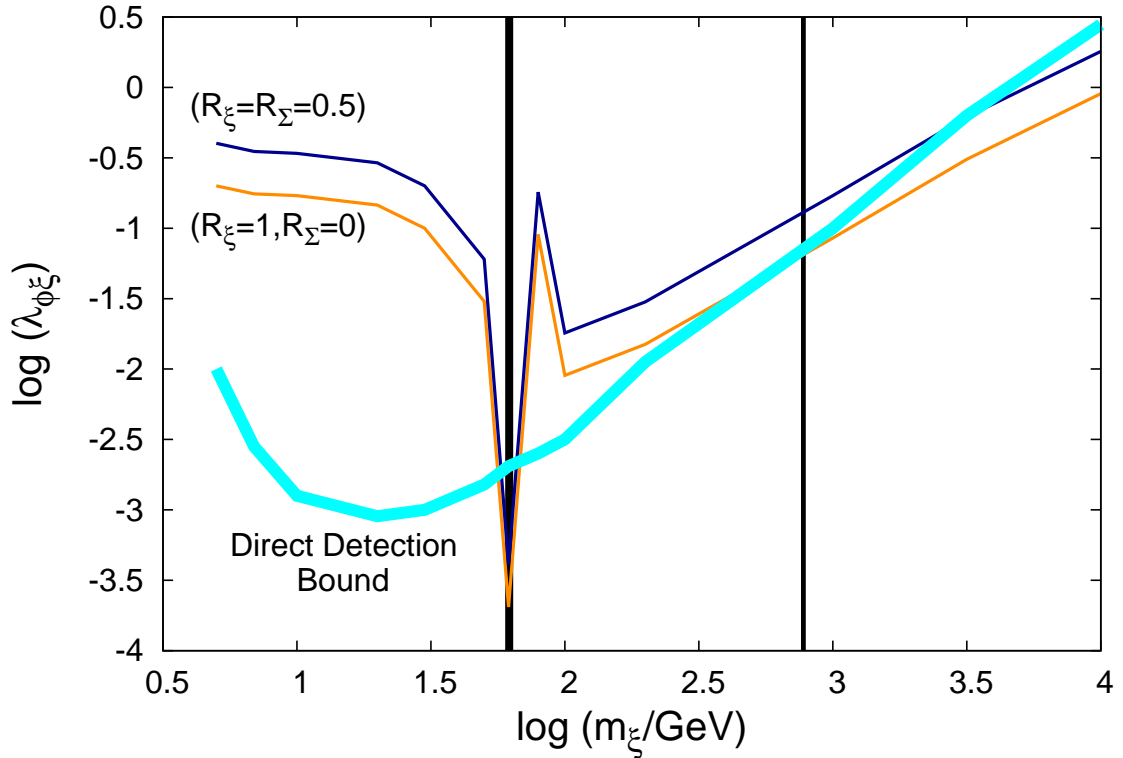


Figure 8: Scalar singlet DM mass predictions from constraints due to indirect searches on M_Σ , observed relic density [5, 7], and direct detection cross section bounds (green curve): (i) Yellow curve, $(R_\xi \approx 1, R_\Sigma \approx 0)$, $500 \text{ GeV} \leq M_\Sigma < 1000 \text{ GeV}$; (ii) Blue curve, $(R_\xi = R_\Sigma \approx 0.5)$, $M_\Sigma = 1.5$ TeV. Common value of ξ mass as low as $m_\xi = 62$ GeV for both the yellow and the blue curves is indicated by the first vertical line. The second vertical line indicates prediction of $m_\xi = 790$ GeV when $R_\xi = 1$ and $\lambda_{\phi\xi} \approx 0.08$. The crossing of the blue line with the green band indicates prediction of a heavier $m_\xi \approx 3.1$ TeV with $\lambda_{\phi\xi} \approx 0.56$ when $R_\xi \approx 0.5$.

In Fig.8 the points on the yellow curve or the blue curve which are also below the green band are allowed by both

the relic density as well as the bounds on the DM-nucleon annihilation cross section as reported by the direct detection experiments. From the Fig.8 we find that for both the yellow and the blue curves, the scalar singlet DM with masses $m_\xi = 10 - 60$ GeV and $65 \leq m_\xi/\text{GeV}$ are ruled out by the combined constraints of relic density and direct detection limits. For small DM-Higgs portal coupling $\lambda_{(\phi,\xi)} \simeq (10^{-4} - 10^{-3})$, the lowest predicted value of the scalar DM mass is $m_\xi \simeq 62$ GeV which is shown by the first vertical solid line in Fig. 8.

We further note that in the case of the yellow curve all scalar DM masses $m_\xi \geq 790$ GeV satisfy the combined constraints due to relic density and direct detection limits. Out of this latter set of solutions, the lowest allowed mass in this range is $m_\xi \simeq 790$ GeV having the DM-Higgs portal coupling $\lambda_{(\phi,\xi)} \simeq 0.08$. These predictions are presented in Table 9.

Table 9: Prediction of singlet scalar component dark matter mass from constraints due to indirect searches, observed DM relic density, and elastic cross section bounds from direct detection experiments. For renormalisation group running, initial values of SM gauge couplings $g_i (i = Y, 2L, 3C)$ and the top-quark Yukawa coupling h_t have been fixed at top quark mass $\mu = m_{top} = 173.34$ GeV using PDG data [125]. The SM Higgs quartic coupling has been fixed at $\lambda_\phi = 0.129$ corresponding to physical Higgs mass $m_h = 125$ GeV [28, 34].

$M_\Sigma(\text{GeV})$	R_ξ	R_Σ	m_ξ (GeV)	$\lambda_{\phi\xi}$	λ_ξ	g_{1Y}	g_{2L}	g_{3C}	h_t
500 – 1000	1.0	0.0	62	$1.7 \times 10^{-4} - 1.6 \times 10^{-3}$	0.25	0.35	0.64	1.16	0.96
500 – 1000	1.0	0.0	790	0.08	0.19	0.35	0.64	1.16	0.96
1500	0.5	0.5	62	$1.7 \times 10^{-4} - 1.6 \times 10^{-3}$	0.25	0.35	0.64	1.16	0.96
1500	0.5	0.5	3100	0.56	0.27	0.35	0.64	1.16	0.96

In the case of the blue curve representing nearly 50% of observed relic density due to ξ (the other $\simeq 50\%$ being due to Σ), while one of the possible m_ξ predictions is similar to the case (a) with $m_\xi \simeq 62$ GeV, the heavier mass solution has been shifted to $m_\xi \geq 3.1$ TeV as indicated by the crossing point of this curve with the green band in Fig. 8. In fact the heavier ξ mass prediction appears to depend upon R_ξ . Consistency of all M_Σ values with direct detection bounds have been already discussed above.

7. Grand unification advantage in dark matter predictions

In the TTM investigations without any GUT origin, the most convenient DM embedding was a scalar singlet DM of mass $\simeq 1.3$ GeV [34]. In addition to fulfilling the constraints due to relic density and direct detection cross section bounds, the higher value of the scalar singlet DM mass prediction was a consequence of vacuum stability constraint of the SM Higgs potential that existed in the TTM without this scalar singlet. When TTM is unified into SU(5), we find the necessity of fermionic triplet DM $\Sigma(3, 0, 1)$ in addition to an intermediate mass colour octet fermion $C_F(1, 0, 8)$ for precision gauge coupling unification. Further, the unified model predicts a SM-singlet Higgs scalar S_{24} originating from 24_H of SU(5) which can be easily made to have an intermediate mass $M_S \simeq (10^8 - 10^9)$ GeV. As such, the corresponding threshold effect due to this scalar ensures vacuum stability for all classes of solutions for leptogenesis and type-II seesaw ansatz for neutrino masses in the TTM unified SU(5). This intermediate mass Higgs scalar guarantees vacuum stability with all allowed values of fermionic triplet DM masses discussed above. However, the class of lighter mass fermion triplet DM predicted by coupling unification being inadequate for relic density, requires the introduction of a scalar singlet DM ξ through $SU(5) \times Z_2$. Thus the GUT theory providing an alternative solution for vacuum stability through the intermediate mass Higgs scalar, now permits much lower mass solutions for the scalar DM component $m_\xi \simeq 62$ GeV and $m_\xi \simeq 790$ GeV which were ruled out by the TTM without grand unification [34].

For heavier $M_\Sigma \simeq 1500$ GeV allowed by indirect search constraints, the GUT embedding of TTM also predicts the lighter scalar DM mass almost identical to $m_\xi \simeq 62$ GeV, although a heavier mass $m_\xi \simeq 3.1$ TeV is also predicted with $\lambda_{\phi,\xi} \simeq 0.56$. These solutions indicate that the heavier m_ξ prediction is a consequence of the value of M_Σ which controls the value of R_ξ . Details of such investigations would be reported elsewhere [126].

The radiative stability of the Higgs mass which has been shown to be possible in TTM even without its GUT embedding [34], is also consistently realised in this SU(5) model which permits [76, 77] fine-tuning of parameters in the presence of radiative corrections.

8. Summary and outlook

This grand unification program is a natural follow up of a recent investigation [34] where it has been shown that the two heavy scalar triplet model (TTM) [30, 32] can successfully explain the current neutrino oscillation data with hierarchical neutrino masses in concordance with cosmological bounds [5, 35] while predicting the observed baryon asymmetry of the Universe through unflavoured or partially flavoured ($\equiv \tau$ -flavoured) leptogenesis without requiring any right-handed neutrino (RHN). Noting that: (i) unlike SO(10) or E_6 , the SU(5) grand unified theory does not have RHNs in its fundamental fermion representations suiting to the basic requirement of the two-triplet model (TTM), and (ii) SU(5) needs smaller representations $15_{H1} \oplus 15_{H2}$ compared to much larger representations $126_{H1} \oplus 126_{H2} \subset$ SO(10) (or $351'_{H1} \oplus 351'_{H2} \subset E_6$), for the first time through this work we have delineated the outstanding position of SU(5) compared to higher rank GUTs to achieve TTM unification.

In addition to a colour octet fermion $C_F(1, 0, 8)$ of mass $M_{C_F} \geq 10^8$ GeV, the unification completion is found to predict the well known fermionic triplet dark matter $\Sigma(3, 0, 1)$ in the mass range $M_\Sigma \sim \mathcal{O}(500 - 3000)$ GeV both of which originate from the non-standard fermionic representation $24_F \subset$ SU(5). Every input value of Σ mass in the investigated range $M_\Sigma \simeq \mathcal{O}(500 - 3000)$ GeV with suitable combinations of masses $M_{C_F}, M_{\Delta_1} = M_{15_{H1}}, M_{\Delta_2}$, and M_U is found to achieve successful unification of all the six different solutions of the ununified TTM of Table 3. On the basis of WIMP DM paradigm, the unification solutions achieved as a function of M_Σ have been categorised into two classes. Under class (i) solutions applicable for heavier $M_\Sigma > 2$ TeV, resonance mass of dominant fermionic DM accounts for the entire value of the observed cosmological relic density. Examples of class (i) solutions corresponding to a chosen resonance mass value of $M_\Sigma = 2.4$ TeV are presented numerically in Table 7 where all the six ununified TTM solutions derived in [34] have been successfully unified through SU(5). Precision gauge coupling unification and proton lifetime estimations as a function of V_{eff} have been presented in Fig. 4 and Fig. 6 under this class (i) solution corresponding to $M_\Sigma = 2.4$ TeV. However, such resonance mass values $M_\Sigma \simeq 2.4$ TeV, or heavier, appear to have been challenged by a number of indirect search experiments as summarised in Sec.5.0.3 and Sec. 6. Then, barring such indirect search constraints, future collider searches may decide on the existence of such a dominant fermionic DM which would go in favour of our class (i) solutions.

A substantial region of our successful precision unification results consists of class (ii) solutions with lighter subdominant DM Σ masses $M_\Sigma \simeq \mathcal{O}(500 - 2000)$ GeV which are not constrained by indirect experimental search results. As these lighter masses can not account for the entire value of the observed cosmological relic density, the resulting deficit is circumvented by the introduction of a scalar singlet DM ξ . Consistent with the combined constraints of observed relic density and direct detection cross section bounds, we have carried out the scalar singlet mass (m_ξ) predictions in relation to M_Σ under indirect search constraints. In the region $M_\Sigma = (500 - 1000)$ GeV where Σ has negligible relic density contribution, this scalar singlet ξ mass is predicted to be $m_\xi \simeq 62$ GeV for a smaller Higgs portal coupling $\lambda_{\phi\xi} = (10^{-4} - 10^{-3})$ or $m_\xi = 790$ GeV for more reasonable value of $\lambda_{\phi\xi} \simeq 0.08$. These lighter ξ -DM masses, which were prevented in the ununified TTM [34] because of the latter's underlying vacuum stability constraint [34], are now permitted through the SU(5) grand unification that provides an alternative solution for the SM vacuum stability. Under indirect search constraint we have examined the case of $M_\Sigma = 1500$ GeV which contributes nearly 50% to the observed cosmological relic density (the other $\simeq 50\%$ being due to ξ). Although the lighter m_ξ and the correspondingly associated smaller values of $\lambda_{\phi\xi}$ remain almost identical as shown in Table 9, the heavier mass prediction is shifted to $m_\xi \simeq 3.1$ TeV. Our investigations clearly indicate that the heavier scalar singlet DM mass prediction (other than $m_\xi = 62$ GeV) can be controlled by M_Σ while respecting indirect search constraints. Details of investigation currently in progress in search of lighter $m_\xi (< 3.1$ TeV) predictions with reasonable values of $\lambda_{\phi\xi}$ will be reported elsewhere [126].

An example of unification solutions under class (ii) category for $M_\Sigma = 500$ GeV is presented through Table 6, Fig. 2, Fig. 3, and Fig. 5. As in the case of class (i) unification results enumerated in Table 7, our class (ii) solutions numerically presented in Table 6 also successfully unify all the six different respective ununified TTM solutions of Table 3 and [34].

We have further shown a comparison through Fig. 7 elucidating how spin-independent $\Sigma - p$ elastic cross section predictions [96] for both the lighter or heavier Σ masses in the range $M_\Sigma \simeq \mathcal{O}(500 - 3000)$ GeV, belonging to both class

(i) and class (ii) solutions, are consistent with direct detection cross section bounds determined experimentally [9, 10].

The vacuum stability of the SM scalar potential in all types of solutions under class (i) or class (ii) is also ensured within the purview of the present SU(5) unification framework through threshold effect of an intermediate mass scalar ($M_{S_{24}} \simeq 10^8 - 10^9$ GeV) originating from the GUT breaking. All the colour octet fermion masses needed to complete gauge coupling unification under both class (i) and class (ii) solutions are noted to satisfy the desired cosmological bound [83].

Even though the present SU(5) model solutions have somewhat lower unification scales, $M_U \simeq O(10^{15})$ GeV, they are associated with an unknown mixing parameter V_{eff} in the proton decay width formula [54, 55, 73] which prevents proton lifetime to be predictive for $p \rightarrow e^+ \pi^0$ mode; rather observation of proton decay is expected to fix this model parameter. In this work we have discussed how the current Hyper-Kamiokande limit partially constrains this parameter space. However, a substantial region of the parameter space with $V_{eff} < 1$ is noted to survive despite improved accuracy in proton lifetime measurements. Any smaller changes over the predominantly one-loop RG determination of unification scales presented here would be similarly consistent with Hyper-Kamiokande limit on the proton lifetime through correspondingly adjusted values of V_{eff} .

In conclusion we find that the present SU(5) GUT framework is quite effective for precision gauge coupling unification, fitting neutrino oscillation data, explaining the observed cosmological baryon asymmetry of the Universe through leptogenesis, and understanding the WIMP DM matter paradigm while ensuring vacuum stability of the SM scalar potential.

9. Acknowledgement

M. K. P. acknowledges financial support through the research project SB/S2/HEP-011/2013 awarded by the Department of Science and Technology, Government of India. R. S. is financed under Ph.D. research fellowship grant of Siksha 'O' Anusandhan, Deemed to be University.

10. Appendix

10.1. Lighter weak triplet and colour octet fermion masses

For the present purpose, we utilize the most convenient Yukawa Lagrangian including both normalizable as well as non-renormalizable (NR) terms [58, 74]

$$\begin{aligned} \mathcal{L}_{NR} &= M_F Tr(24_F^2) + Y_{24} Tr(24_F^2 24_H) \\ &+ \frac{1}{M_{NR}} [k_1 Tr(24_F^2) Tr(24_H^2) + k_2 [Tr(24_F 24_H)]^2] \\ &+ k_3 Tr(24_F^2 24_H^2) + k_4 Tr(24_F 24_H 24_F 24_H) \end{aligned} \quad (86)$$

For the mass scale in the non-renormalizable term we use $M_{NR} = M_{String} \sim 10^{17}$ (or $M_{NR} \simeq 10^{18}$ GeV = reduced Planck scale). When the Yukawa couplings are switched off, all component fermions in 24_F are near the GUT scale with degenerate mass M_F . When SU(5) is broken by the VEV

$$\langle S_{24H} \rangle = \frac{V_U}{\sqrt{30}} \text{diag}(2, 2, 2, -3, -3) \quad (87)$$

with $V_U \sim M_{GUT}$, all component fermions in 24_F are expected to split in their masses [74]

$$\begin{aligned}
M_{(LQ)_F} &= M_F - \frac{Y_{24}V_U}{2\sqrt{30}} + \frac{V_U^2}{M_{NR}} \left(k_1 + \frac{(13k_3 - 12k_4)}{60} \right), \\
M_{S_F} &= M_F - \frac{Y_{24}V_U}{\sqrt{30}} + \frac{V_U^2}{M_{NR}} \left(k_1 + \frac{7}{30}(k_3 + k_4) \right), \\
M_\Sigma &= M_F - \frac{3Y_{24}V_U}{\sqrt{30}} + \frac{V_U^2}{M_{NR}} \left(k_1 + \frac{3}{10}(k_3 + k_4) \right), \\
M_{C_F} &= M_F + \frac{2Y_{24}V_U}{\sqrt{30}} + \frac{V_U^2}{M_{NR}} \left(k_1 + \frac{2}{15}(k_3 + k_4) \right)
\end{aligned} \tag{88}$$

Our RG constraints on gauge coupling unification need $M_\Sigma \sim 500 - 1000$ GeV, but $M_{C_F} \sim 10^8 - 10^9$ GeV compared to GUT scale values of $M_F \sim V_U \sim \mathcal{O}(10^{16})$ GeV. We discuss below how with appropriate fine tuning of parameters in eq.(88), these two desired masses can be made lighter than the GUT scale while keeping other component masses in 24_F super heavy near $\simeq M_U$. For the lightest weak triplet fermion mass we use

$$\begin{aligned}
M_\Sigma &\simeq \frac{3V_U^2}{10M_{NR}}(k_3 + k_4), \\
&\simeq \mathcal{O}(500 - 1000) \text{ GeV},
\end{aligned} \tag{89}$$

Then using the first relation of eq.(89) in the third relation of eq.(88) gives

$$M_F - \frac{3Y_{24}V_U}{\sqrt{30}} + \frac{V_U^2}{M_{NR}}k_1 \sim 0. \tag{90}$$

Then using eq.(88), eq.(89), and eq.(90) gives

$$\begin{aligned}
M_{C_F} &= \frac{5Y_{24}V_U}{\sqrt{30}} + \frac{4}{9}M_\Sigma \\
&\simeq \frac{5Y_{24}V_U}{\sqrt{30}},
\end{aligned} \tag{91}$$

where the second line follows from the fact that $M_\Sigma \ll M_{C_F}$ which is desired for our unification solutions discussed in Sec. 3. Now we get $M_{C_F} = \mathcal{O}(10^8 - 10^9)$ GeV for Yukawa coupling values $Y_{24} \simeq 10^{-7} - 10^{-5}$. Noting that $k_3 + k_4 \simeq 0$ and utilising relations given under eq.(89), eq.(90), and eq.(91) in the corresponding expressions under eq.(88), it is straight forward to show that all component masses of 24_F become super heavy except Σ and C_F as noted above.

References

- [1] G. L. Fogli, E. Lisi, A. Marrone, D. Montanino, A. Palazzo and A. M. Rotunno, Phys. Rev. D **86**, 013012 (2012) [arXiv:1205.5254 [hep-ph]]; T. Schwetz, M. Tortola and J. W. F. Valle, New J. Phys. **13**, 063004 (2011) [arXiv:1103.0734 [hep-ph]].
- [2] D. V. Forero, M. Tortola and J. W. F. Valle, Phys. Rev. D **90**, no.9, 093006 (2014) [arXiv:1405.7540 [hep-ph]]; M. C. Gonzalez-Garcia, M. Maltoni and T. Schwetz, Nucl. Phys. B **908**, 199-217 (2016) [arXiv:1512.06856 [hep-ph]].
- [3] I. Esteban, M. C. Gonzalez-Garcia, A. Hernandez-Cabezudo, M. Maltoni and T. Schwetz, JHEP **01**, 106 (2019) [arXiv:1811.05487 [hep-ph]].
- [4] D. N. Spergel *et al.* [WMAP], Astrophys. J. Suppl. **148**, 175-194 (2003) [arXiv:astro-ph/0302209 [astro-ph]]; E. Komatsu *et al.* [WMAP], Astrophys. J. Suppl. **180**, 330-376 (2009) [arXiv:0803.0547 [astro-ph]]; G. Hinshaw *et al.* [WMAP], Astrophys. J. Suppl. **180**, 225-245 (2009) [arXiv:0803.0732 [astro-ph]]; E. Komatsu *et al.* [WMAP], Astrophys. J. Suppl. **192**, 18 (2011) [arXiv:1001.4538 [astro-ph.CO]].
- [5] P. A. R. Ade *et al.* [Planck], Astron. Astrophys. **571**, A16 (2014) [arXiv:1303.5076 [astro-ph.CO]]; P. A. R. Ade *et al.* [Planck], Astron. Astrophys. **594**, A13 (2016) [arXiv:1502.01589 [astro-ph.CO]].
- [6] F. Zwicky, Helv. Phys. Acta, **6** (1933) 110; D. N. Spergel *et al.* (WMAP Collaboration), Astrophys. J. Suppl. **170** (2007) 377; J. Einasto, arXiv: 0901.0632[astro-ph.CO]; G. R. Blumenthal, S. M. Faber, J. R. Primack and M. J. Rees, Nature **311**, 517-525 (1984); J. Angle *et al.* (XENON10 Collaboration), Phys. Rev. Lett **107**, 051301 (2011); *ibid.* Phys. Rev. Lett **110**, 249901 (2013), arXiv: 1104.3088 [astro-ph.CO]; L. E. Strigari, Phys. Rept. **531**, 1-88 (2013) [arXiv:1211.7090 [astro-ph.CO]].

- [7] WMAP Collaboration, D. N. Spergel et al, *Astrophys. J. Suppl.* **170** (2007)377 [astro-ph/0603449] [INSPIRE]; D. Larson, J. Dunkley, G. Hinshaw, E. Komatsu, M. R. Nolta, C. L. Bennett, B. Gold and M. Halpern *et al.*, *Astrophys. J. Suppl.* **192**, 16 (2011), arXiv:1001.4635 [astro-ph.CO].
- [8] D. S. Akerib *et al.* [LUX Collaboration], *Phys. Rev. Lett.* **118**, no. 2, 021303 (2017) [arXiv:1608.07648 [astro-ph.CO]].
- [9] E. Aprile *et al.* [XENON Collaboration], *Phys. Rev. Lett.* **119**, no. 18, 181301 (2017) [arXiv:1705.06655 [astro-ph.CO]].
- [10] E. Aprile *et al.* [XENON Collaboration], *Phys. Rev. Lett.* **121**, no. 11, 111302 (2018) [arXiv:1805.12562 [astro-ph.CO]].
- [11] X. Cui *et al.* [PandaX-II Collaboration], *Phys. Rev. Lett.* **119**, no. 18, 181302 (2017) [arXiv:1708.06917 [astro-ph.CO]].
- [12] B. W. Lee, S. Weinberg, *Phys. Rev. Lett.* **39** (1977) 165 [INSPIRE]; K. Griest, M. Kamionkosky, *Phys. Rev. Lett.* **64** (1990) 615 [INSPIRE].
- [13] P. Athron *et al.* [GAMBIT], *Eur. Phys. J. C* **77**, no.8, 568 (2017) [arXiv:1705.07931 [hep-ph]].
- [14] J. C. Pati, A. Salam, *Phys. Rev. D* **8** (1973) 1240; J. C. Pati, A. Salam, *Phys. Rev. D* **10** (1974) 275.
- [15] H. Georgi and S. L. Glashow, *Phys. Rev. Lett.* **32** (1974) 438.
- [16] H. Georgi, *in Particles and Fields*, Williamsburg, Virginia (1974), AIP Conf. Proc. **23** (1975) 575; H. Fritzsch and P. Minkowski, *Ann. Phys.* **93** (1975) 193.
- [17] F. Gursev, P. Ramond, P. Sikivie, *Phys. Lett. B* **69** (1976) 177; Y. Achiman and B. Steck, *Phys. Lett. B* **77** (1978) 389; Q. Shafi, *Phys. Lett. B* **79** (1978) 301; R. Barbieri, D. V. Nanopoulos, *Phys. Lett. B* **91** (1980) 369; F. Gursev and M. Serdaroglu, *Nuo. Cim.* **65A** (1981) 337.
- [18] Darwin Chang, R. N. Mohapatra, M. K. Parida, *Phys. Rev. Lett.* **52** (1984) 1072; Darwin Chang, R. N. Mohapatra, M. K. Parida, *Phys. Rev. D* **30** (1984) 1052; Darwin Chang, R. N. Mohapatra, M. K. Parida, *Phys. Lett. B* **142** (1984) 55-58; M. K. Parida, *Phys. Rev. D* **78** (2008) 053001 arXiv:0804.4571[hep-ph].
- [19] M. K. Parida, R. Samantaray, *Eur.Phys. J. ST* **229** (2020) no.21, 3243-3262 arXiv:2002.06869 [hep-ph].
- [20] P. Minkowski, *Phys. Lett. B* **67**, 421-428 (1977); M. Gell-Mann, P. Ramond and R. Slansky, in *Supergravity*, edited by P. van Nieuwenhuizen and D. Freedman, (North-Holland, 1979), p. 315; S.L. Glashow, in *Quarks and Leptons*, Cargèse, eds. M. Lévy et al., (Plenum, 1980, New-York), p. 707; T. Yanagida, in *Proceedings of the Workshop on the Unified Theory and the Baryon Number in the Universe*, edited by O. Sawada and A. Sugamoto (KEK Report No. 79-18, Tsukuba, 1979), p. 95; R. N. Mohapatra and G. Senjanovic, *Phys. Rev. Lett.* **44**, 912 (1980)
- [21] J. Schechter and J. W. F. Valle, *Phys. Rev. D* **22**, 2227 (1980).
- [22] W. Konetschny and W. Kummer, *Phys. Lett. B* **70** (1977) 433; M. Magg and C. Wetterich, *Phys. Lett. B* **94** (1980) 61; T. P. Cheng, L. F. Li, *Phys. Rev. D* **22** (1980) 2860; G. Lazarides, Q. Shafi and C. Wetterich, *Nucl. Phys. B* **181** (1981) 287; R. N. Mohapatra, G. Senjanovic, *Phys. Rev. D* **23** (1981) 165; J. Schechter, J. W. F. Valle, *Phys. Rev. D* **25** (1982) 774.
- [23] R. Foot, L. Lew, X. G. He and G. C. Joshi, *Z. Phys. C* **44** (1989) 441; E. Ma, *Phys. Rev. Lett.* **81** (1998) 1171 [arXiv:hep-ph/9805219].
- [24] V. A. Kuzmin, V. A. Rubakov and M. E. Shaposhnikov, *Phys. Lett. B* **191**, 171-173 (1987).
- [25] M. Fukugita and T. Yanagida, *Phys. Lett. B* **174**, 45-47 (1986).
- [26] S. Davidson, E. Nardi and Y. Nir, *Phys. Rept.* **466**, 105-177 (2008) [arXiv:0802.2962 [hep-ph]].
- [27] M. K. Parida, B. P. Nayak, R. Satpathy and R. L. Awasthi, *JHEP* **1704** (2017) 075 arXiv:1608.03956[hep-ph].
- [28] M. Chakraborty, M. K. Parida and B. Sahoo, *JCAP* **01**, 049 (2020) arXiv:1906.05601 [hep-ph].
- [29] A. S. Josphipura, E. A. Paschos and W. Rodejohann, *JHEP* **08**, 029 (2001) [arXiv:hep-ph/0105175 [hep-ph]]; A. S. Josphipura, E. A. Paschos, W. Rodejohann, *JHEP* **0108** (2001) 029 [arXiv: hep-ph/0105175[hep-ph]].
- [30] E. Ma and U. Sarkar, *Phys. Rev. Lett.* **80**, 5716 (1998) [hep-ph/9802445].
- [31] R. Gonzalez Felipe, F. R. Joaquim and H. Serodio, *Int. J. Mod. Phys. A* **28** (2013) 1350165 [arXiv:1301.0288[hep-ph]].
- [32] D. Aristizabal Sierra, M. Dhen and T. Hambye, *JCAP* **1408**, 003 (2014) [arXiv:1401.4347 [hep-ph]].
- [33] D. Aristizabal Sierra, F. Bazzocchi, I. de Medeiros Verzilaz, *Nucl. Phys. B* **858** (2012) 196, arXiv:1112.1843[hep-ph]. D. Aristizabal Sierra, L. A. Munoz, E. Nardi, *Phys. Rev. D* **80** (2009) 016007; D. Aristizabal Sierra, M. Losado, E. Nardi, *JCAP* **0912** (2009) 015, arXiv:0905.0662.
- [34] M. K. Parida, M. Chakraborty, S. K. Nanda, R. Samantaray, *Nucl. Phys. B* **960** (2020) 115203 arXiv:2005.12077[hep-ph].
- [35] S. Vagnozzi *et al.*, *Phys. Rev. D* **94** (2016) 083522, arXiv:1605.04320[astro-ph.CO], S. Vagnozzi *et al.*, *Phys. Rev. D* **96** (2017) 123503, arXiv:1701.08172[astro-ph.CO], S. Vagnozzi *et al.*, *Phys. Rev. D* **98** (2018) 123526, arXiv:1802.08694[astro-ph.CO].
- [36] Planck Collaboration, N. Aghanim et al., Planck 2018 results. I. Overview and the cosmological legacy of Planck, *Astron. Astrophys.* **641** (2020) A1, [1807.06205].
- [37] Planck Collaboration, N. Aghanim et al., Planck 2018 results. VI. Cosmological parameters, *Astron. Astrophys.* **641** (2020) A6, [1807.06209].
- [38] B. Bajc, G. Senjanovic and F. Vissani, *Phys. Rev. Lett.* **90** (2003) 051802.
- [39] H. S. Goh, R. N. Mohapatra and S. P. Ng, *Phys. Lett. B* **570** (2003) 215.
- [40] R. N. Mohapatra, M. K. Parida and G. Rajasekaran, *Phys. Rev. D* **69**, 053007 (2004); R. N. Mohapatra, M. K. Parida and G. Rajasekaran, *Phys. Rev. D* **71**, 057301 (2005); R. N. Mohapatra, M. K. Parida and G. Rajasekaran, *Phys. Rev. D* **72**, 013002 (2005); K. R. S. Balaji, A. S. Dighe, R. N. Mohapatra, and M. K. Parida, *Phys. Rev. Lett.* **84** (2000) 5034-5037 [arxiv:hep-ph/0001310].
- [41] A. S. Josphipura and K. M. Patel, AIP Conf. Proc. **1382** (2011) 163-167; A. S. Josphipura, K. M. Patel, *Phys. Rev. D* **83** (2011) 095002 [arXiv:1102.5148[hep-ph]].
- [42] M. K. Parida, *Phys. Rev. D* **78** (2008) 053004 [arXiv:0804.4571[hep-ph]].
- [43] T. Hambye and G. Senjanovic, *Phys. Lett. B* **582**, 73-81 (2004) [arXiv:hep-ph/0307237 [hep-ph]].
- [44] T. Hambye, K. Kannike, E. Ma and M. Raidal, *Phys. Rev. D* **75**, 095003 (2007) [arXiv:hep-ph/0609228 [hep-ph]].
- [45] T. Hambye, M. Raidal and A. Strumia, *Phys. Lett. B* **632**, 667-674 (2006) [arXiv:hep-ph/0510008 [hep-ph]].
- [46] T. Hambye, *New J. Phys.* **14**, 125014 (2012) [arXiv:1212.2888 [hep-ph]].
- [47] P. H. Gu, E. Ma and U. Sarkar, *Phys. Rev. D* **94**, no.11, 111701 (2016) [arXiv:1608.02118 [hep-ph]].
- [48] T. Rink, W. Rodejohann and K. Schmitz, arXiv:2006.03021[hep-ph].
- [49] S. K. Majee, M. K. Parida, A. Raychaudhuri, U. Sarkar, *Phys. Rev. D* **75** (2007) 075003; S. K. Majee, M. K. Parida, A. Raychaudhuri, *Phys. Lett. B* **668** (2008) 299-302 [arXiv:0807.3959[hep-ph]]; M. K. Parida, A. Raychaudhuri, *Phys. Rev. D* **82** (2010) 093007 [arXiv:1007.5085[hep-ph]].

- [50] T. Ohlsson, M. Pernow, E. Sonnerlind, Eur. Phys. J. **C80** (2020) **no.11**, 1089 [arXiv:2006.1393[hep-ph]]; D. Meloni, T. Ohlsson, M. Pernow, Eur. Phys. J. **C80** (2020) 840 [arXiv:1911.11411[hep-ph]].
- [51] G. Domenech, M. Goodsell, C. Wetterich, JHEP **2101** (2021) 180 [arXiv:2008.04310[hep-ph]].
- [52] R. Slansky, Phys. Rep. **79** (1979) 1-128.
- [53] Pran Nath and P. Fileviez Perez, Phys. Rep. **441** (2007) 191-317 [arxiv:hep-ph/0601023].
- [54] P. Fileviez Perez, C. Murugui, A. D. Plascencia, JHEP **11** (2019) 093 [arXiv:1908.01772[hep-ph]].
- [55] P. Fileviez Perez, A. Gross and C. Murugui, Phys. Rev. **D 98** (2018) 075032 arXiv:1804.07831[hep-ph].
- [56] H. S. Goh, R. N. Mohapatra, S. Nasri, Phys. Rev. **D 70** (2004) 075022 arXiv:hep-ph/0408139.
- [57] R. N. Mohapatra, M. K. Parida, Phys. Rev. **D 84** (2011) 095021 arXiv:1109.2188[hep-ph].
- [58] B. Bajc, M. Nemevsek and G. Senjanovic, Phys. Rev. D 76 (2007) 055011 sw[arXiv:hep-ph/0703080].
- [59] M. Cirelli, N. Forengo, A. Strumia, Nucl. Phys. **B753** (2006) 178 arXiv:hep-ph/0512090.
- [60] M. Cirelli, A. Strumia and M. Tamburini, Nucl. Phys. **B 787** (2007) 152 arXiv:0706.4071[hep-ph].
- [61] E. Ma, D. Suematsu, Mod. Phys. Lett. **A 24** (2009) 583-589 arXiv:0809.0942[hep-ph].
- [62] M. Cirelli, R. Franceschini, A. Strumia, Nucl. Phys. **B 800** (2008) 204 arXiv:0802.3378[hep-ph].
- [63] R. Franceschini, T. Hambye, A. Strumia, Phys. Rev. **D 78** (2008) 033002 arXiv:0805.1613[hep-ph].
- [64] M. Frigerio and T. Hambye, Phys. Rev. **D 81** (2010) 075002 [arXiv:0912.1545[hep-ph]].
- [65] M. K. Parida, P. K. Sahu, K. Bora, Phys. Rev. **D 83** (2011) 093004 [arXiv:1011.4577[hep-ph]][INSPIRE].
- [66] J. Elias-Miro, J. R. Espinosa, G. F. Giudice, H. M. Lee and A. Strumia, JHEP **06**, 031 (2012) [arXiv:1203.0237 [hep-ph]].
- [67] K. Abe *et al.* [Super-Kamiokande Collaboration], Phys. Rev. **D 95** (2017) **no.1**, 012004 [arXiv:1610.03597[hep-ex]].
- [68] M. Yokoyama [Hyper-Kamiokande Proto Collaboration], "The Hyper-Kamiokande Experiment", in Proceedings, *Prospects in Neutrino Physics (NuPhys2016)*: London, U. K. Dec.12-14, 2016,2017 [arXiv:1705.00306[hep-ex]].
- [69] J. Beringer *et al.* [Particle Data Group], Phys. Rev. D **86**, 010001 (2012); C. Patrignani *et al.* (Particle Data Group), Chin. Phys. **C40** (2016) no.10, 100001, 01;
- [70] I. Dorsner and P. Fileviez Perez, Nucl. Phys. **B 723** (2005) 53 [arXiv:hep-ph/0504276]; I. Dorsner, P. Fileviez Perez and R. Gonzalez Felipe, Nucl. Phys. **B 747** (2006) 312 [arXiv:hep-ph/0512068].
- [71] M. K. Parida, Mainak Chakraborty, Biswonath Sahoo, Adv. High Energy Phys. **2018** (2018) 4078657 arXiv:1804.01803[hep-ph]; M. K. Parida and Rajesh Satpathy, Adv. High Energy Phys. **2019** (2019) 3572682 arXiv:1809.06612[hep-ph].
- [72] M. K. Parida, Phys. Lett. **B 704** (2011) 206-2011 ,arXiv:1106.4137[hep-ph].
- [73] P. Fileviez Perez, Phys. Lett. **B 654** (2007) 189 arXiv:hep-ph/0702287; P. Fileviez Perez, H. Iminniyaz and G. Rodrigo, Phys. Rev. **D 78** (2008) 015013 [arXiv:0803.4156[hep-ph]]; I. Dorsner and P. Fileviez Perez, JHEP 0706 (2007) 029 [arXiv:hep-ph/0612216].
- [74] B. Bajc and G. Senjanovic, JHEP 0708 (2007) 014 [arXiv:hep-ph/0612029]; B. Bajc, I. Dorsner, M. Nemevsek, JHEP 11 (2008) 007, arXiv:0809.1069[hep-ph].
- [75] M. L. Kynshi, M. K. Parida, Phys. Rev. **D 47** (1993) R4830-R4834.
- [76] F. del Aguilla, L. E. Ibanez, Nucl. Phys. **B 177** (1981) 60.
- [77] R. N. Mohapatra, G. Senjanovic, Phys. Rev. **D 27** (1983) 1601.
- [78] H. Georgi, H. R. Quinn, S. Weinberg, Phys. Rev. Lett. **33** (1074) 451.
- [79] D. R. T. Jones, Phys. Rev. **D 25** (1982) 581.
- [80] D. Chang, R. N. Mohapatra, J. Gipson, R. E. Marshak, M. K. Parida, Phys. Rev. **D 31** (1985) 1718.
- [81] P. Langacker, N. Polonsky, Phys. Rev. **D 47** (1993) 4028 [hep-ph/9210235]. arXiv:....
- [82] M. K. Parida and B. D. Cajee, Eur. Phys. J. **C 44** (2005) 447-457 [arXiv:hep-ph/0507030].
- [83] N. Arkani-Hamed and S. Dimopoulos, JHEP 0506 (2005) 073 [arXiv:hep-th/0405159].
- [84] A. J. Buras, J. Ellis, M. K. Gaillard, D. V. Nanopoulos, Nucl. Phys. B 135 (1978) 66; T. J. Goldman, D. A. Ross, Nucl. Phys. B 171 (1980) 273; J. Ellis, D. V. Nanopoulos, S. Rudaz, Nucl. Phys. B 202 (1982) 43; L. E. Ibanez, C. Munoz, Nucl. Phys. B 245 (1984) 425; C. Munoz, Phys. Lett. B 177 (1986) 45.
- [85] L. F. Abbot, M. B. Wise, Phys. Rev. D 22 (1980) 2208.
- [86] Y. Aoki, C. Dawson, J. Noaki, A. Soni, Phys. Rev. D 75 (2007) 014507, arXiv:hep-lat/0607002; Y. Aoki *et al.* , Phys. Rev. D 78 (2008) 054505 [arXiv:0806.1301 [hep-lat]].
- [87] Y. Aoki, E. Shintani and A. Soni, Phys. Rev. **D 89** (2014) **no.1**,014505 [arXiv:1304.7424[hep-lat]].
- [88] Y. Aoki, T. Izubuchi, E. Shintani and A. Soni, Phys. Rev. **D 96** (2017) 014526 [arXiv:1705.01338[hep-ph]].
- [89] A. Hryczuk, I. Cholis, R. Inigo, M. Tavakoli and P. Ullio, JCAP **1407** 031 (2014) arXiv:1401.6212[hep-ph].
- [90] M. Cirelli, F. Sala and M. Taoso, JHEP **1410** (2014) 033 [Erratum-ibid.**1501** (2015) 041][arXiv:1407.7058 [hep-ph]].
- [91] A. G. Delannoy, B. Dutta, A. Gurrola, W. Johns *et al.*, Phys. Rev. Lett. **111** (2013) 061801 [arXiv:1304.7779][hep-ph]].
- [92] E. W. Kolb and M. S. Turner, Front. Phys. **69**, 1 (1990).
- [93] G. Bertone, D. Hooper and J. Silk, Phys. Rept. **405** (2005) 279 [hep-ph/0404175].
- [94] P. Gondolo and G. Gelmini, Nucl. Phys. **B 360**, 145 (1991).
- [95] J. Hisano, S. Matsumoto, M. Nagai, O. Saito and M. Senami, Phys. Lett. **646** (2007) 34 [arXiv:hep-ph/0610249].
- [96] J. Hisano, K. Ishiwata and N. Nagata, JHEP **1506** (2015) 097 [arXiv:1504.00915[hep-ph]].
- [97] J. Billard, L. Strigari and E. Figuera-Feliciano, Phys. Rev. **D 89** (2014) 023524.
- [98] F. del Aguilla and J. A. Aguilar-saavedra, Nucl. Phys. **B 813** (2009) 22 arXiv: 0808.2468[hep-ph].
- [99] A. Arhrib, B. Bajc, D. K. Ghosh, T. Han, I. Puljak and G. Senjanovic, Phys. Rev. **D 82** (2010) 053004.
- [100] A. De Roeck *et al.*, Eur. Phys. J C 66 (2010) 525 [arXiv:0909.3240[hep-ph]].
- [101] W. Y. Keung and G. Senjanovic, Phys. Rev. Lett. **50** (1983) 1427.
- [102] A. Das, S. Mandal, and T. Modak, Phys. Rev. **D 102** (2020) **no.3**, 033001 [arXiv:2005.02267[hep-ph]].
- [103] M. Boezio *et al.* (PAMELA Collaboration) 2008; O. Adrilani *et al.*(PAMELA Collaboration), Nature **458**, 607 (2009); O. Adrilani *et al.* (PAMELA Collaboration), Phys. Rev. Lett **111**, no.8, 081102 (2013).

- [104] A. A. Abodo et al. (Fermi/LAT Collaboration), Phys. Rev. Lett. **102** (2009) 181101 [[arXiv: 0905.0025 [hep-ex]].
- [105] S. Mohanty, S. Rao, and D. P. Roy, Int. J. Mod. Phys. **A27** (2012) **6**, 1250025 [arXiv:1009.5058[hep-ph]].
- [106] L. Accardo et al. (AMS Collaboration), Phys. Rev. Lett **113**, no. 12, 121101 (2014).
- [107] J. Han, C. S. Frenk, V. R. Eke, L. Gao, S. D. White, arXiv: 1201.1003 [astro-ph.HE].
- [108] A. Hektor, M. Radial, E. Tempel, Astrophys. J. **762**, 22 (2013).
- [109] F. Aharonian (HESS Collaboration) 2009 [arXiv: 0909.0727[hep-ph]].
- [110] J. Aleksy et al. (MAGIC Collaboration), Astrophys. J. **710**, 634 (2010).
- [111] M. Ackermann, M. Ajello, A. Allafort, L. Baldini, J. Ballet, et al. JCAP **1005**, 025 (2010).
- [112] L. Dugger, T. E. Jeltema and S. Profumo, JCAP **1012**, 015 (2010).
- [113] S. Zimer, J. Conrad, and A. Pinzke (Fermi-LAT Collaboration) (2011).
- [114] X. Huang, G. Vertongen, and C. Weniger, JCAP **1201**, 042 (2012).
- [115] E. Komatsu et al. (WMAP Collaboration), Astrophys. J. Suppl. **180**, 330 (2009).
- [116] G. Hinshaw et al. (WMAP Collaboration), Astrophys. J. Suppl. **208**, 19 (2013).
- [117] J. L. Sievers et al. (Atacama Cosmology Telescope), JCAP **1310**, 060 (2013).
- [118] K. Story, C. Reichard, Z. Hou, R. Keisler, K. Aird et al., Astrophys. J. **779**, 86 (2013).
- [119] O. Lebedev, Eur. Phys. J. **C 72** (2012) 2058 [arXiv:1203.0156[hep-ph]].
- [120] Biswonath Sahoo, M. K. Parida and Mainak Chakraborty, Nucl. Phys. **B 938** (2019) 56-113 [arXiv:1707.01286[hep-ph]].
- [121] J. McDonald, Phys. Rev. D **50**, 3637 (1994), hep-ph/0702143.
- [122] W. L. Guo and Y. L. Wu, JHEP **1010**, 083 (2010), arXiv:1006.2518 [hep-ph].
- [123] Q. H. Cao, E. Ma, J. Wudka and C. P. Yuan, arXiv:0711.3881[hep-ph]
- [124] J. M. Cline, K. Kainulainen, P. Scott and C. Weniger, Phys. Rev. D **88**, 055025 (2013) Erratum: [Phys. Rev. D **92**, no. 3, 039906 (2015)] [arXiv:1306.4710 [hep-ph]].
- [125] Particle Data Group, K. A. Olive *et al.*, Chin. Phys. **C 38** (2014) 090001; S. Bethke, Nucl. Phys. Proc. Suppl. **234** (2013) 229 arXiv:1210.0325[hep-ex].
- [126] M. K. Parida and R. Samantaray,(under preparation).